Evaluation of SGV with Particle Flow Emulation in context of the “Point 5” Analysis

Madalina Chera

ILD Software and Analysis Phone Meeting

18.10.2017

Universität Hamburg
DER FORSCHUNG | DER LEHRE | DER BILDUNG

Particles, Strings, and the Early Universe
Collaborative Research Center SFB 676

DESY

SGV: Default JER

- SGV default does not consider Particle Flow confusion effects:

Cluster splitting → energy double counting:

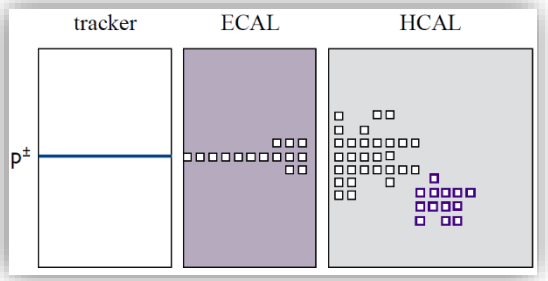

Cluster merging → energy loss:

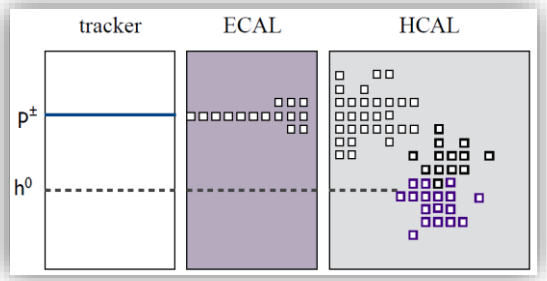

- Performs perfect track-cluster associations (SGV-PERF)
- Investigated JER performance on Z→ uds events:
  - Considered $\sqrt{s}$ ranging from 30 to 500 GeV → 6 different jet energies
  - Compared results to LoI and DBD performance

SGV: Default JER Performance

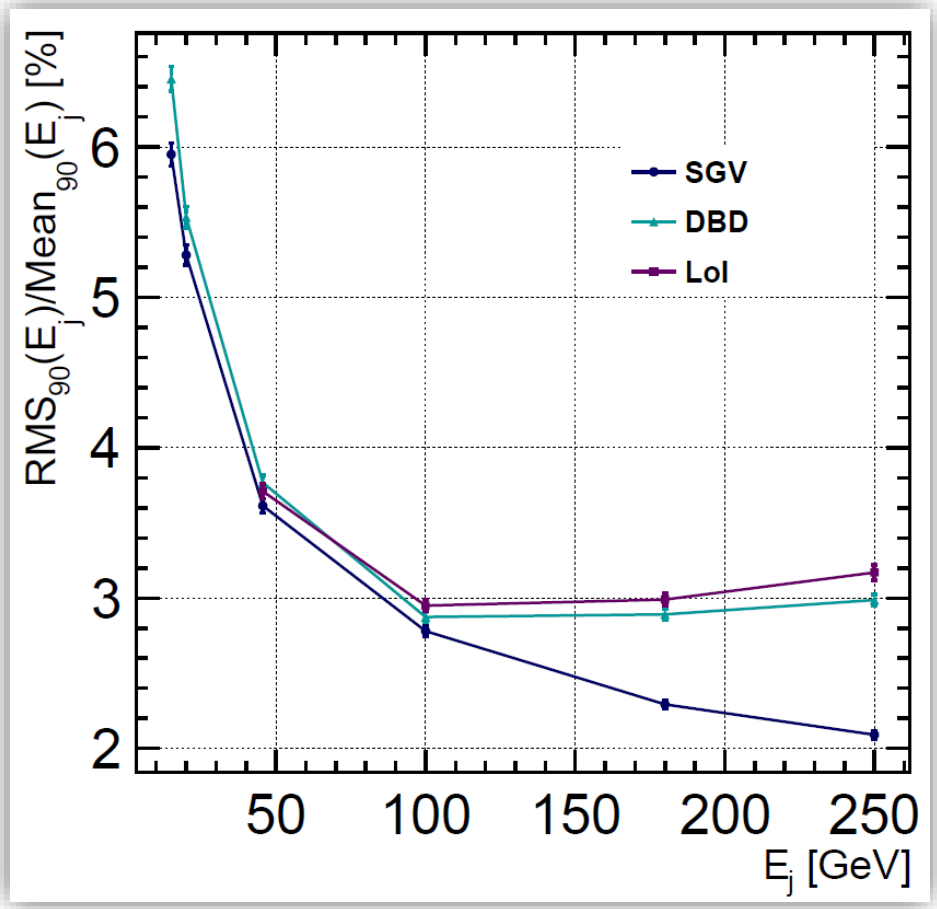

- **Observed**:

→ Good agreement in 45-100 GeV range
→ 8% discrepancy below 45 GeV
→ 30% discrepancy above 150 GeV

JER discrepancies could be addressed by implementing PFlow confusion emulation w.r.t. full simulation behaviour!

SGV with Particle Flow Confusion Emulation

- PandoraPFA confusion studied using 8000 $e^+e^- \rightarrow udsc$ **LoI** events
- Confusion parametrised as:
  - Cluster splitting probability: depends mostly on cluster isolation
  - Probability to split/merge whole cluster: depends only on particle energy
  - Probability to split cluster fraction: fraction depends on energy and isolation
- M. Berggren: LCWS11, Granada and arXiv:1203.0217v1
- Parametrisations implemented in SGV
- Studied SGV (rev86) performance with PFlow confusion (SGV-PFL) implementation using Z→ uds events
  - rev86 = version used in producing SGV SM mass production

SGV with Confusion Emulation: Performance

Visible energy

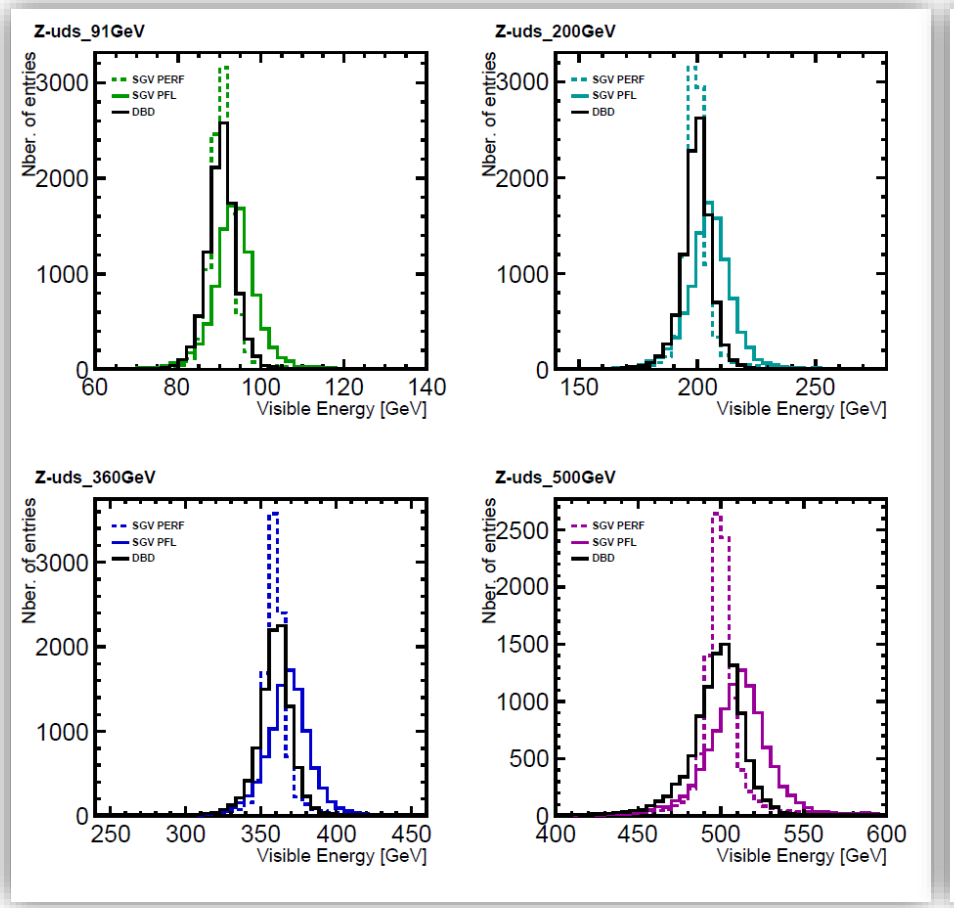

Jet Energy Resolution

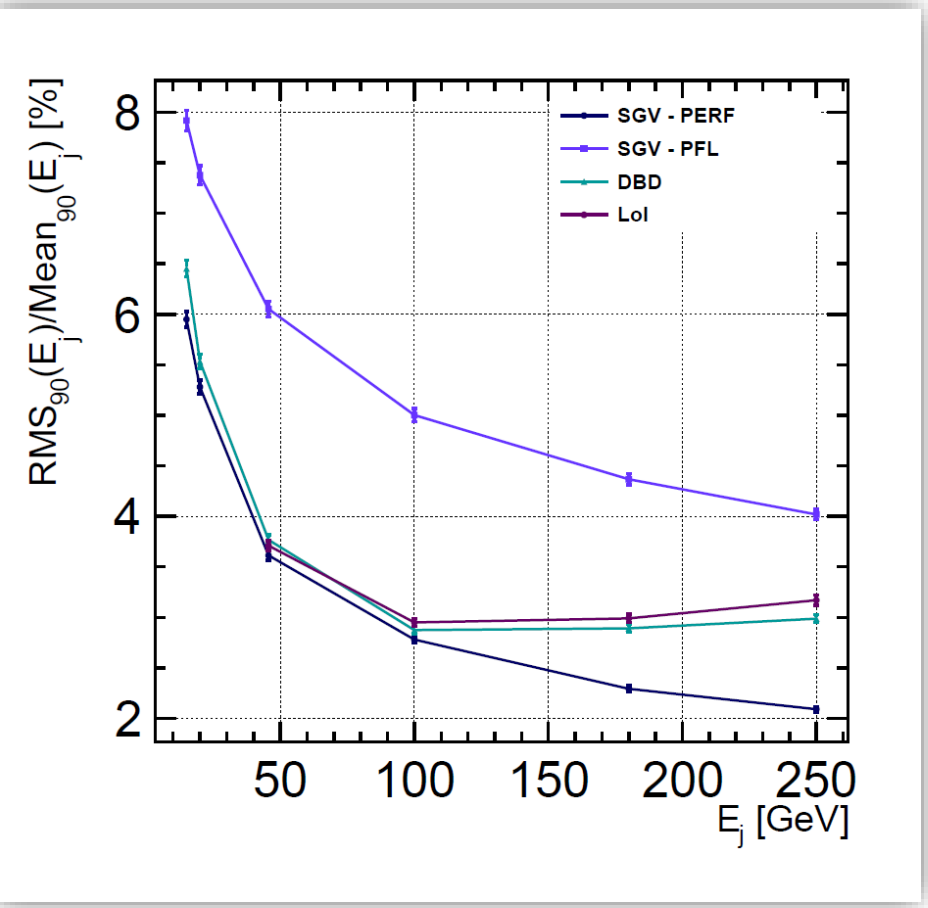

→ **SGV-PFL: JER on average 55% worse than DBD performance.**

→ **Investigated the E_{vis} shift to higher values.**

Visible Energy Study

PFO Charged Energy

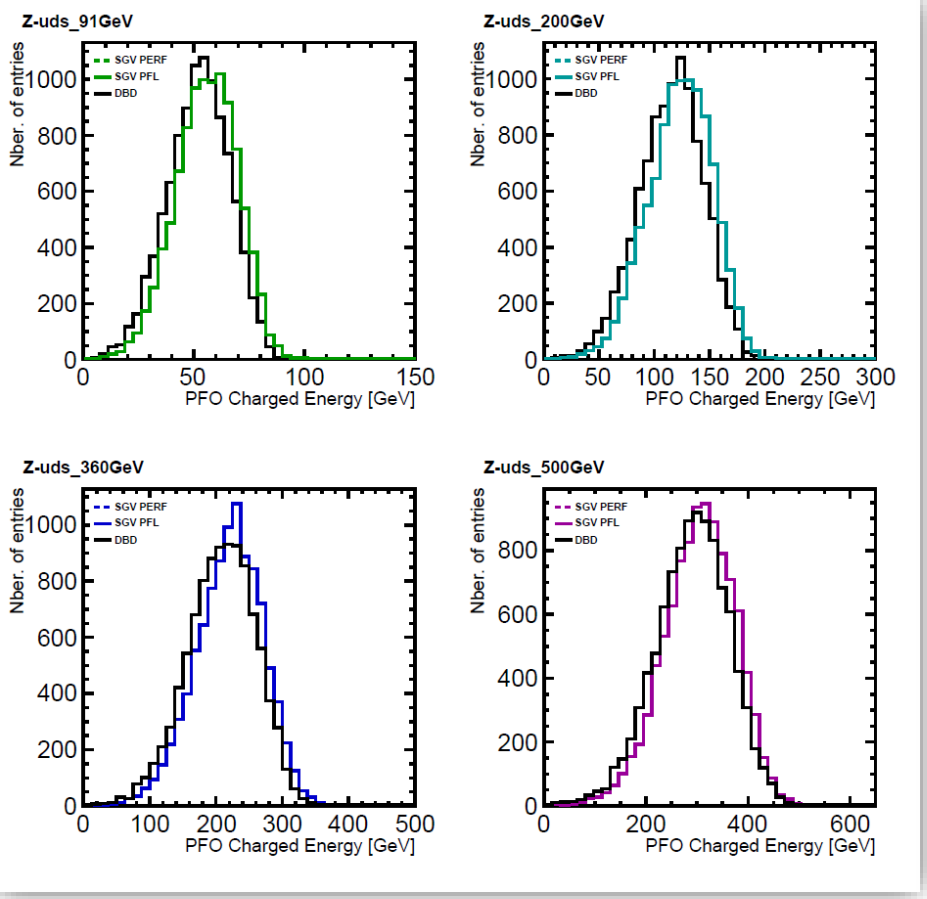

PFO Neutral Energy

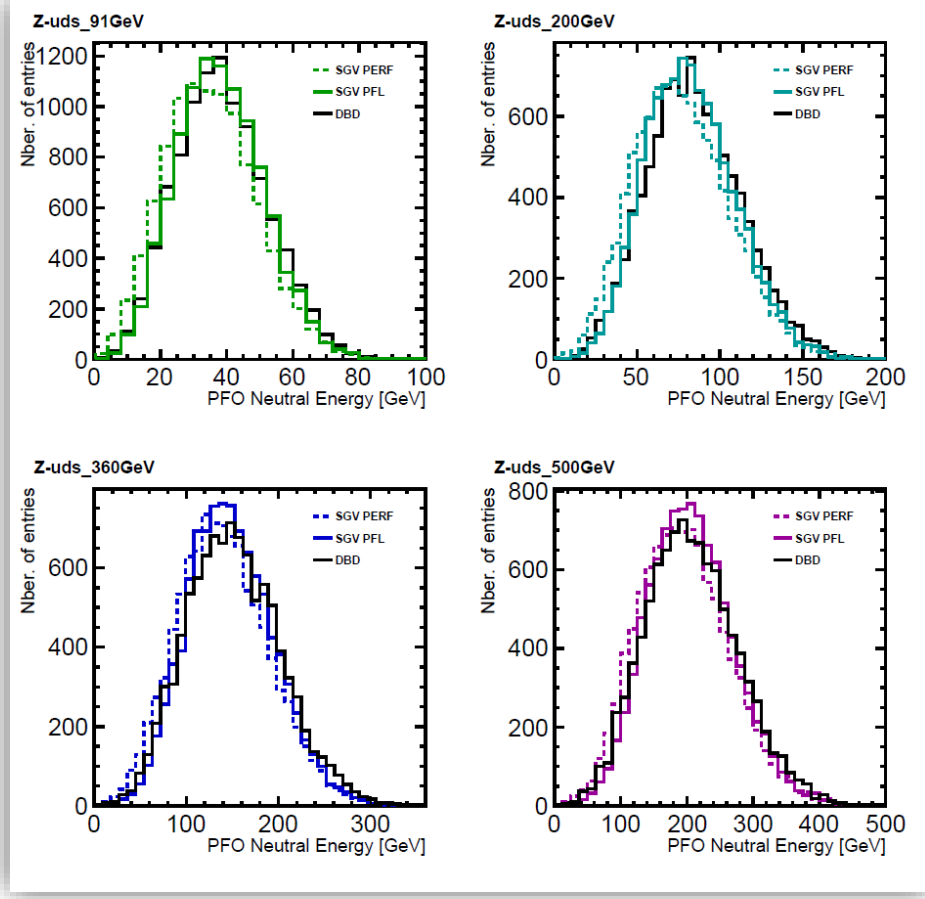

- Culprit: higher neutral PFO energy → possibly more cluster splitting & unbalanced merging.
- **Scale neutral PFO energy down to SGV PERF–like values.**

Neutral PFO Energy Correction

- **Goal**: scale $Mean_{PFL}$ visible energy to $Mean_{PERF} \leftrightarrow Mean_{PERF} = k \cdot Mean_{PFL}$
- Study used 14 $Z \rightarrow uds$ samples with $\sqrt{s}$ ranging from 30 to 500 GeV:
  - Simulated with SGV (rev86) with and without PFlow confusion emulation
- For each sample: E_{vis} distribution fitted with Gaussian → **mean value extracted**

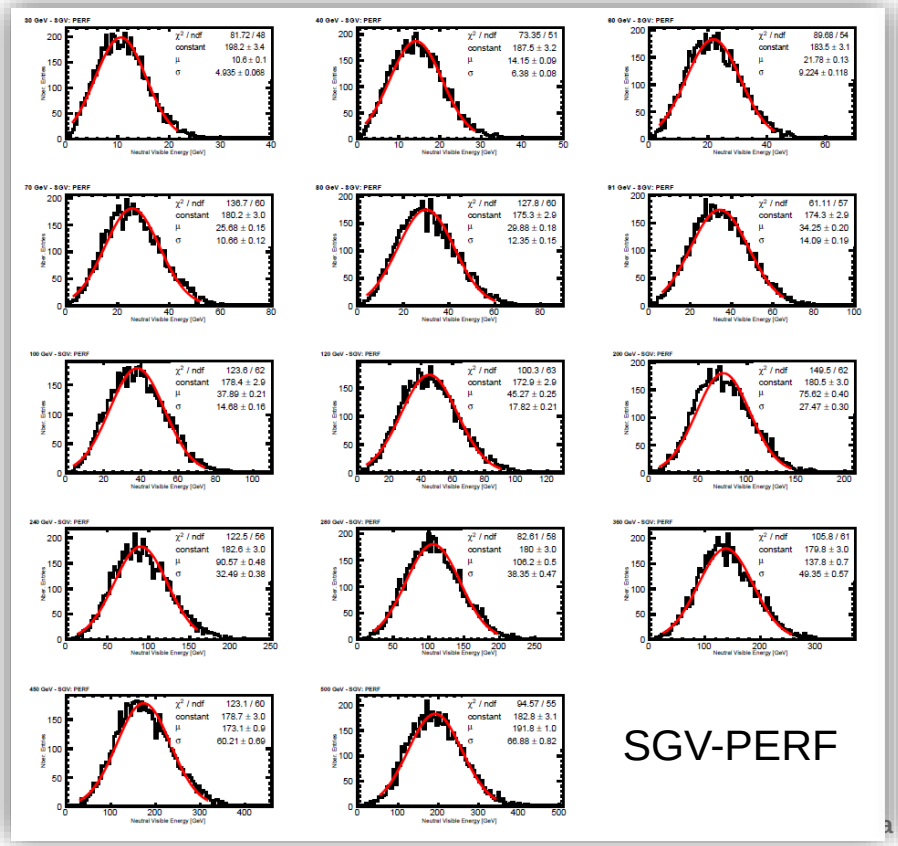

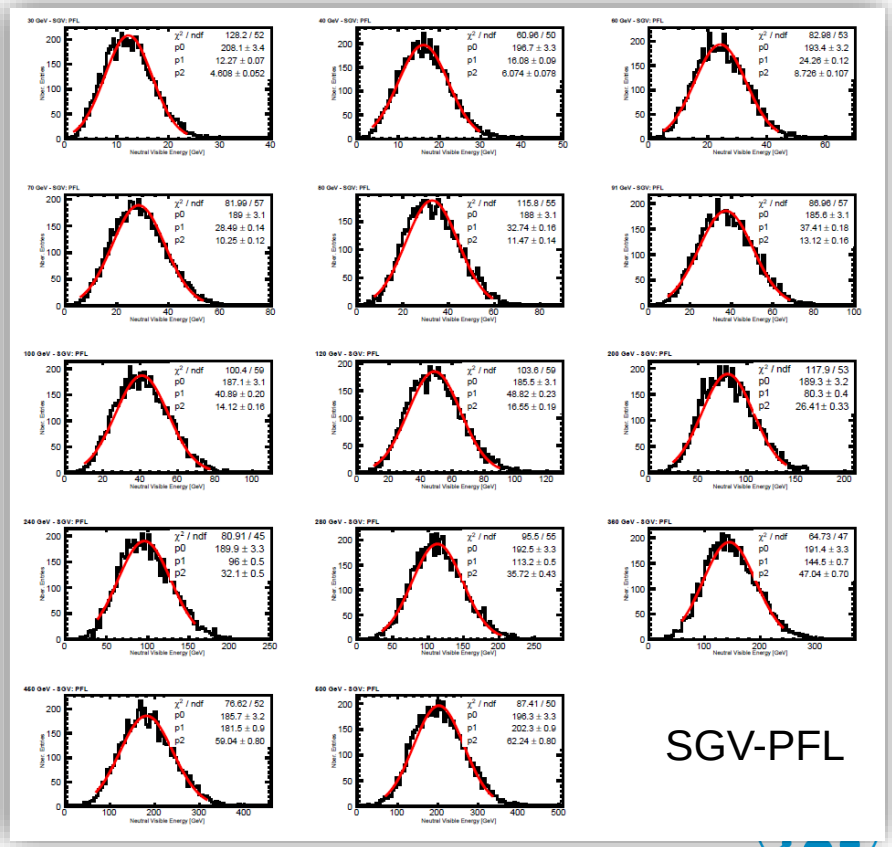

Neutral PFO Energy Correction

- **Goal**: scale $Mean_{PFL}$ visible energy to $Mean_{PERF}$ ↔ $Mean_{PERF} = k \cdot Mean_{PFL}$
- Study used 14 $Z \rightarrow uds$ samples with $\sqrt{s}$ ranging from 30 to 500 GeV:
  - Simulated with SGV (rev86) with and without PFlow confusion emulation
- For each sample: E_{vis} distribution fitted with Gaussian → **mean value extracted**

- **Fitting function: $k(x) = a \cdot x + b \cdot \ln x + c$**
  - Where x = observed visible energy in event
  - Plug in E_{vis} of each SGV-PFL event → obtain k
  - The charged energy is compatible → leave as is
  - Scale energy of each neutral PFO in event by k

- Investigated outcome of neutral energy scaling

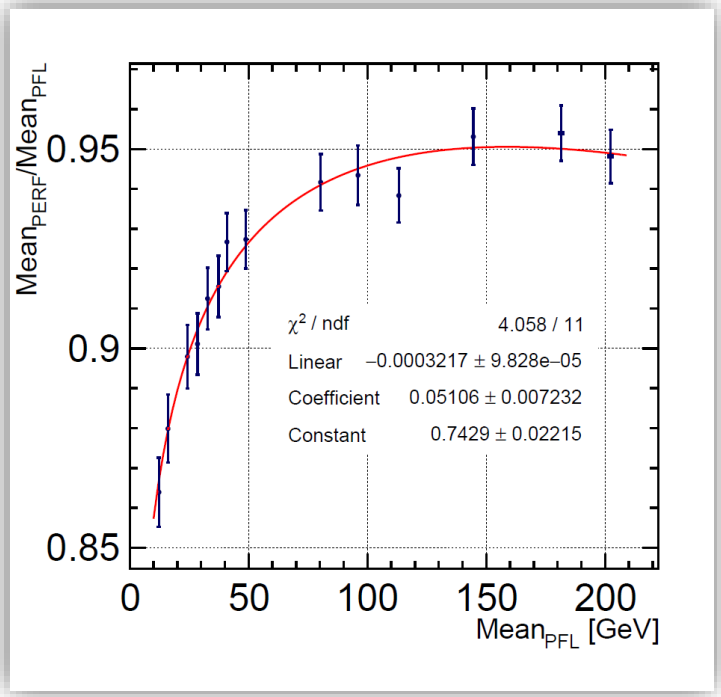

SGV-PFL Performance with Neutral Energy Correction

Visible energy

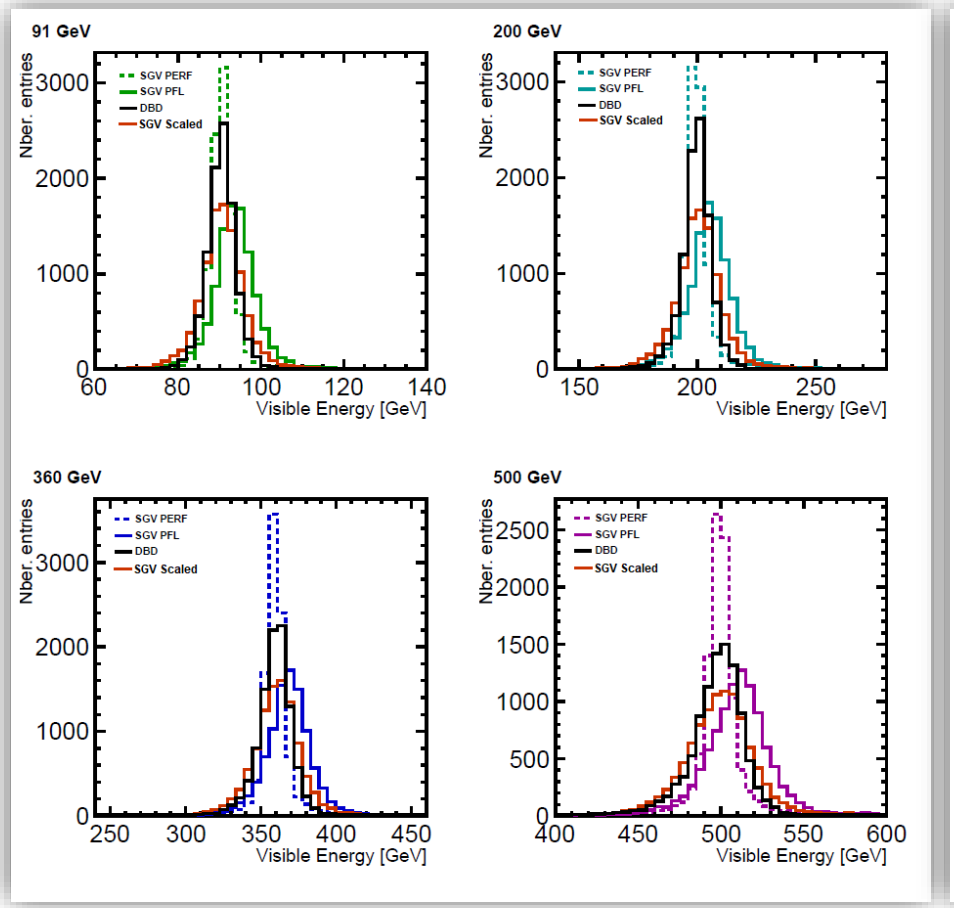

Jet Energy Resolution

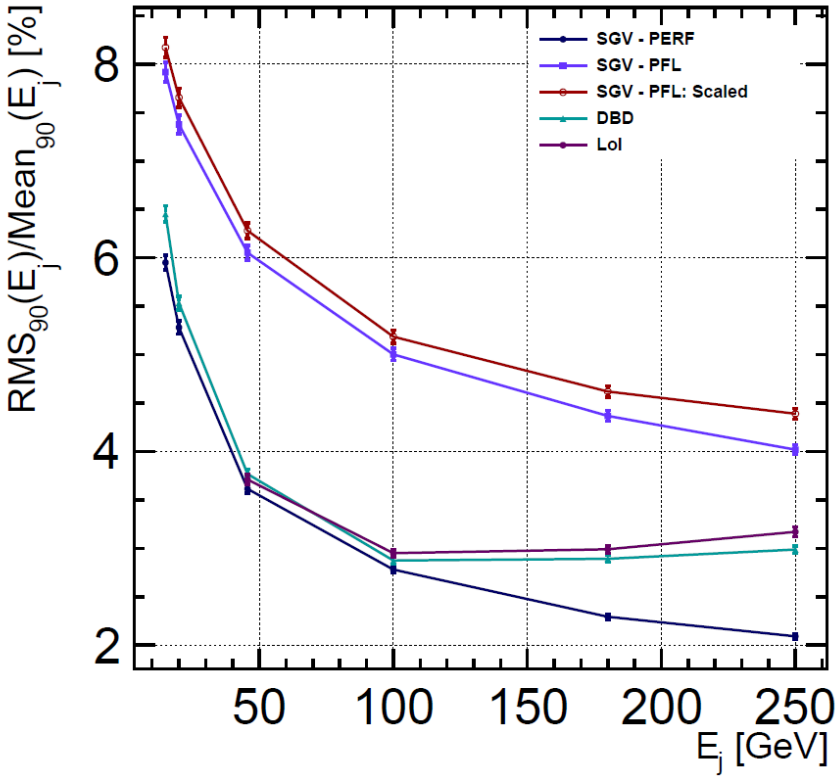

→ E_{vis} central value recovered, however RMS_{90} 1-7% larger.
→ JER 4-9% worse than SGV-PFL (scaling a distribution!).

SGV-PFL Performance with Neutral Energy Correction

Visible energy

Jet Energy Resolution

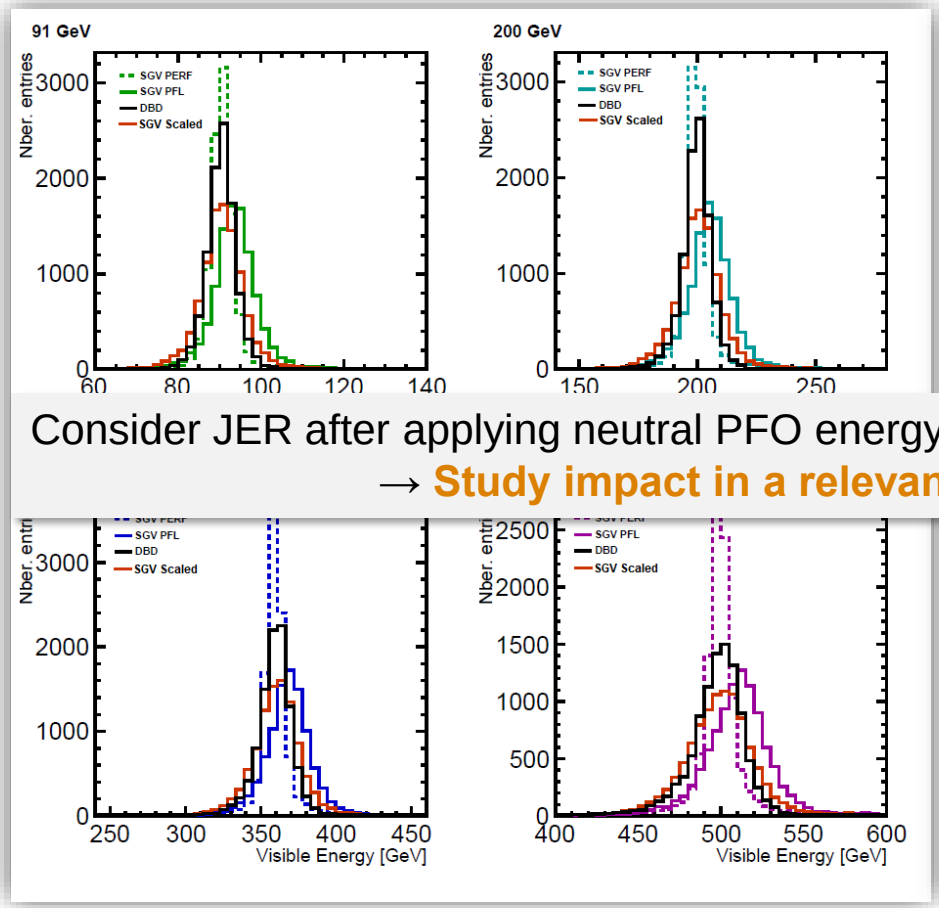

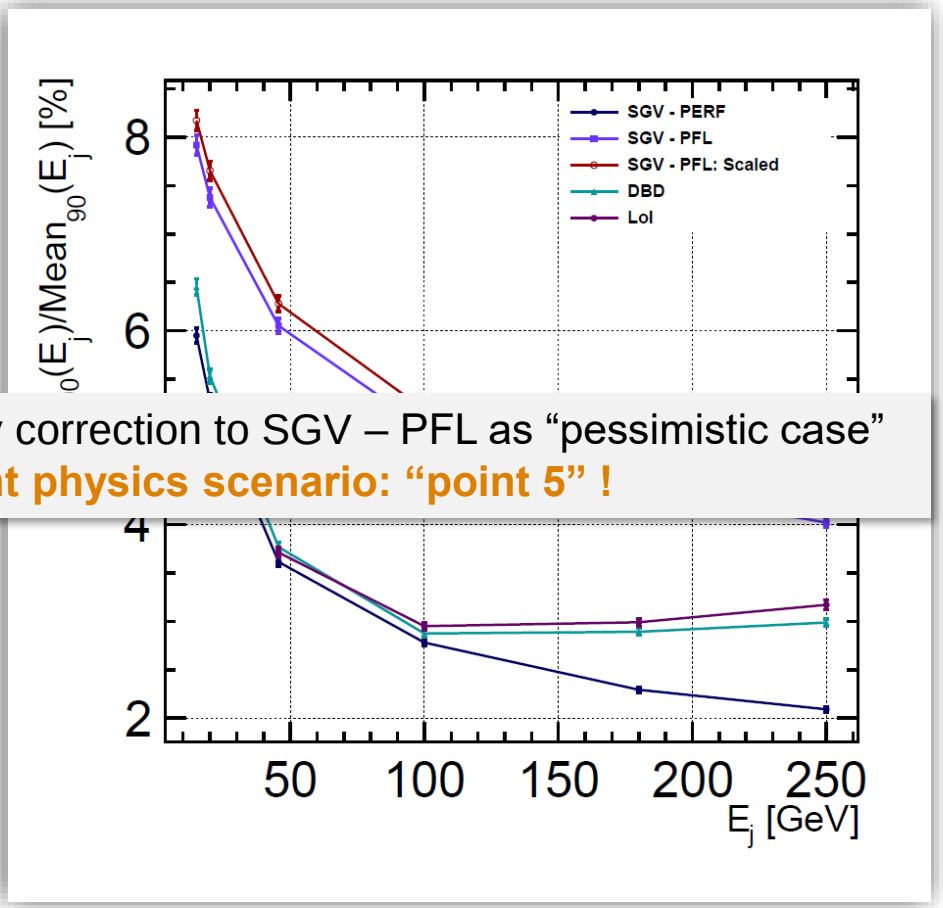

Consider JER after applying neutral PFO energy correction to SGV – PFL as “pessimistic case”

→ **Study impact in a relevant physics scenario: “point 5” !**

→ **E_{vis} central value recovered, however RMS_{90} 1-7% larger.**

→ **JER 4-9% worse than SGV-PFL (scaling a distribution!).**

Reminder: $\tilde{\chi}_1^{\pm}$ and $\tilde{\chi}_2^0$ Pair Production at the ILC

"Point 5" benchmark : gaugino pair production at ILC

http://arxiv.org/pdf/1006.3396.pdf (ILD LoI)
http://arxiv.org/pdf/0911.0006v1.pdf (SiD LoI)

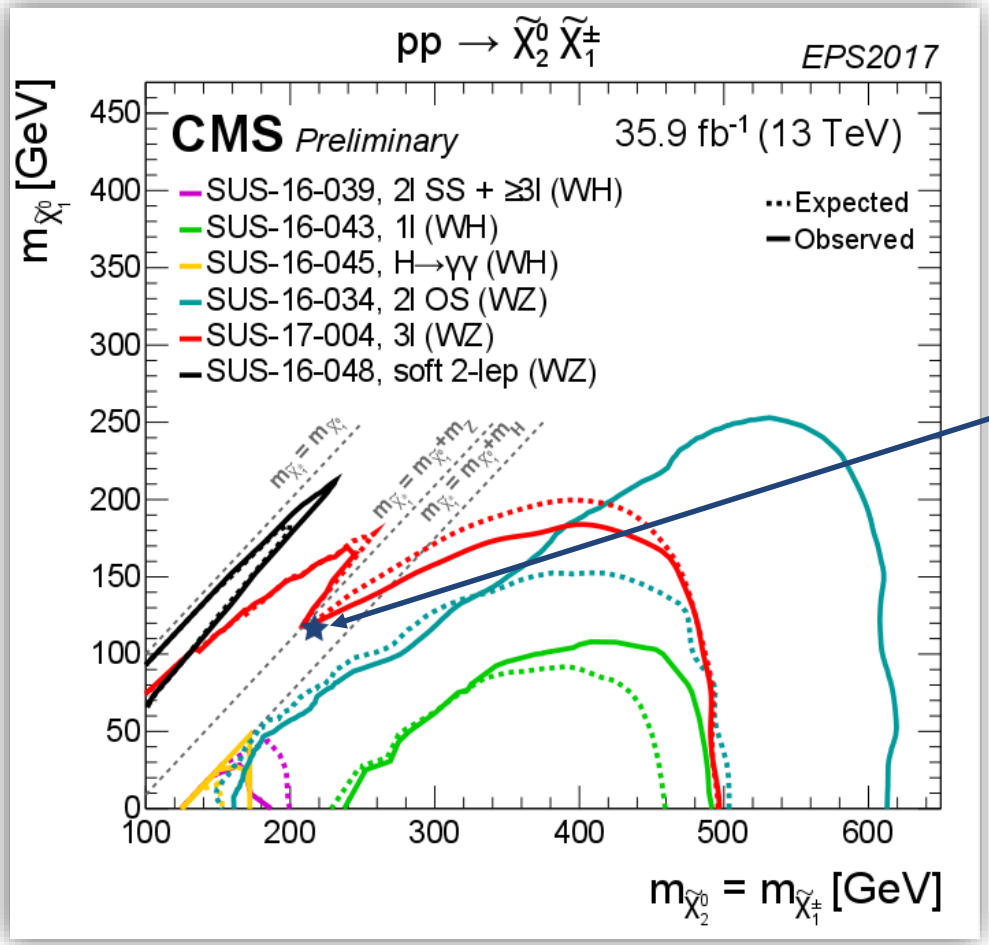

Particle	Mass [GeV]
$\tilde{\chi}_1^0$	115.7
$\tilde{\chi}_1^{\pm}$	216.5
$\tilde{\chi}_2^0$	216.7
$\tilde{\chi}_3^0$	380

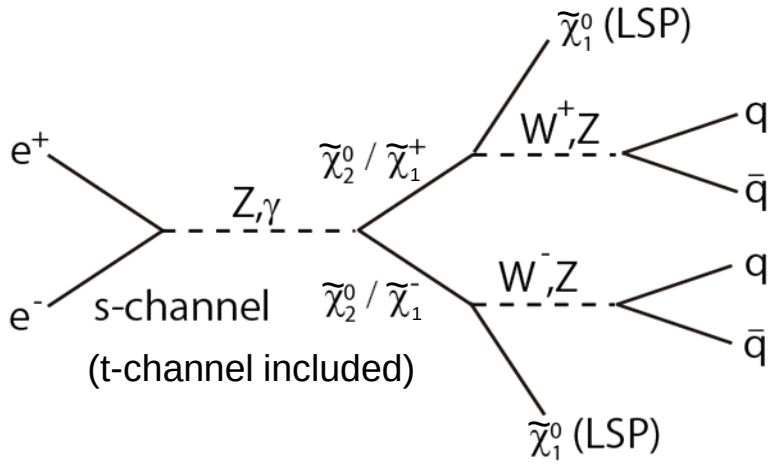

$$\tilde{\chi}_1^{\pm} \to \tilde{\chi}_1^0 W^{\pm} \qquad BR = 99.4\%$$

$$\tilde{\chi}_2^0 \to \tilde{\chi}_1^0 Z^0 \qquad BR = 96.4\%$$

LoI-DBD-SGV(-PFL) "Point 5" Comparison

- "Point 5" SUSY signal and background samples were simulated with SGV-PFL (rev.86)
- Used mass produced SGV-PFL SM background samples
- The neutral PFO energy correction was applied to ALL samples
- Repeated DBD version of the "point 5" analysis on SGV data:
  - Uses a kinematic fit with equal mass constraint (jet pairing)
  - The mass determination procedure presented in detail here
  - The cross-section determination discussed in detail here
  - **Full analysis and LoI-DBD comparison presented at LCWS15**
- This talk → comparison of final results considering:
  - LoI full sim. → the DBD version of the analysis was run on old LoI ntuples
  - DBD full sim.
  - SGV fast sim with PFlow confusion emulation and neutral PFO energy correction

Mass Determination Results Comparison

- Mass difference to LSP ($\tilde{\chi}_1^0$) is **larger** than M_Z → decays of real gauge bosons
- This is a **two-body decay** (well known kinematics!)
- **Use edge values to calculate gaugino masses!**

Sim.	Low edge $\tilde{\chi}_1^\pm$	High edge $\tilde{\chi}_1^\pm$	Low edge $\tilde{\chi}_2^0$	High edge $\tilde{\chi}_2^0$
LOI	80.4 ± 0.2	129.9 ± 0.7	92.3 ± 0.4	128.3 ± 0.9
DBD	79.8 ± 0.3	129.9 ± 1.0	92.2 ± 0.4	128.3 ±0.6
SGV	80.4 ± 0.2	128.6 ± 0.9	92.4 ± 0.3	126.9 ± 1.3

Sim.	$\tilde{\chi}_1^\pm$ Mass [GeV]	$\tilde{\chi}_2^0$ Mass [GeV]	$\tilde{\chi}_1^0$ Mass [GeV]
Model	216.5	216.7	115.7
LOI	216.9 ± 3.20	220 ± 1.4	118.4 ± 1.1
DBD	216.94 ± 3.36	220.45 ± 1.32	118.07 ± 0.9
SGV	217.93 ± 4.84	220.47 ± 1.19	119.63 ± 1.23

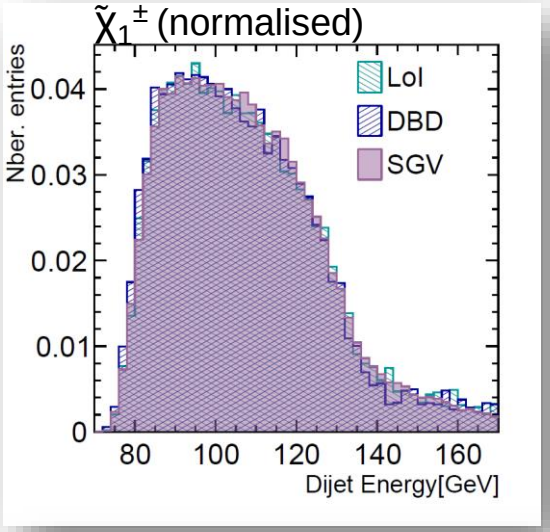

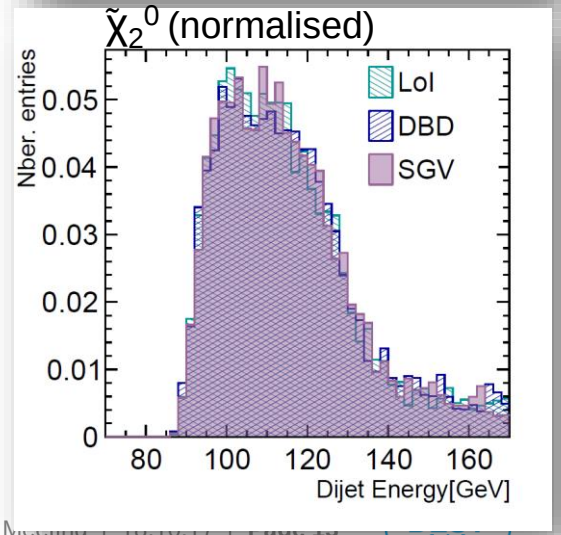

Mass Determination Results Comparison

- Mass difference to LSP ($\tilde{\chi}_1^0$) is **larger** than M_Z → decays of real gauge bosons
- This is a **two-body decay** (well known kinematics!)
- **Use edge values to calculate gaugino masses!**

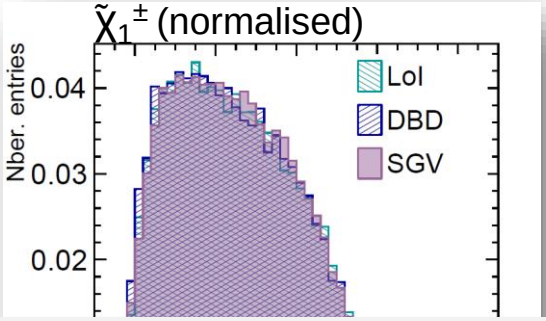

Sim.	Low edge $\tilde{\chi}_1^{\pm}$	High edge $\tilde{\chi}_1^{\pm}$	Low edge $\tilde{\chi}_2^0$	High edge $\tilde{\chi}_2^0$

Observed:

→ **Very similar results for LoI, DBD and SGV-PFL**

→ **Impact of discrepancy in JER not perceptible on analysis level due to:**

- **jet clustering effects**
- **jet pairing confusion**
- **reduced sensitivity due to using kinematic fit**

Sim.	χ_1^- Mass [GeV]	χ_2^0 Mass [GeV]	χ_1^0 Mass [GeV]
Model	216.5	216.7	115.7
LOI	216.9 ± 3.20	220 ± 1.4	118.4 ± 1.1
DBD	216.94 ± 3.36	220.45 ± 1.32	118.07 ± 0.9
SGV	217.93 ± 4.84	220.47 ± 1.19	119.63 ± 1.23

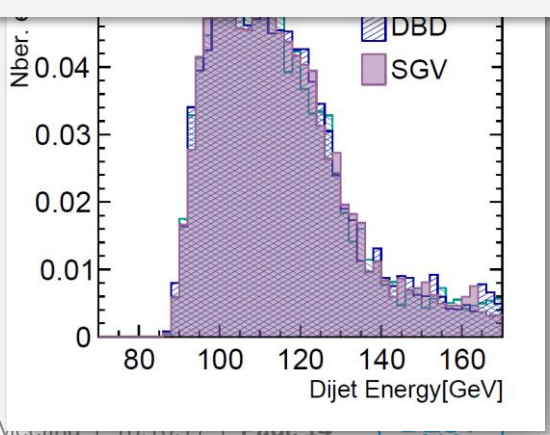

Cross-Section Determination Results Comparison

- Since $\sigma \propto \frac{Nr.events}{\varepsilon \cdot \int \mathcal{L}} \Rightarrow$ the goal is to identify the number of $\tilde{\chi}_1^{\pm}$ and $\tilde{\chi}_2^0$ events from the total dijet mass distribution → **Perform 2D template fit!**

$$f_{Fit}(x,y) = a \cdot f_{\tilde{\chi}_1^{\mp}}(x,y) + b \cdot f_{\tilde{\chi}_2^0}(x,y)$$

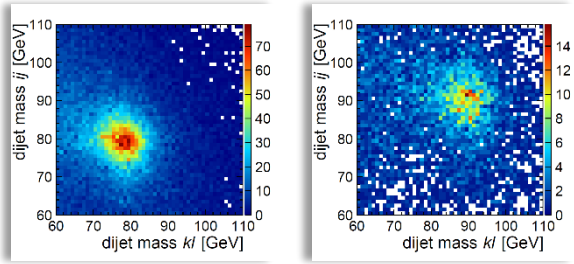

- a and b = the fraction of template events found in the total data distribution (in an ideal case, a = b =1)

Simulation	$\tilde{\chi}_1^{\pm}$ x-section [fb]	$\tilde{\chi}_2^0$ x-section [fb]
Generator level	132.15	22.79
LOI	132.9 ± 1.14	23.17 ± 0.67
Generator level	112.54	19.2
DBD	112.66 ± 0.97	19.28 ± 0.58
SGV	112.56 ± 0.93	19.29 ± 0.56

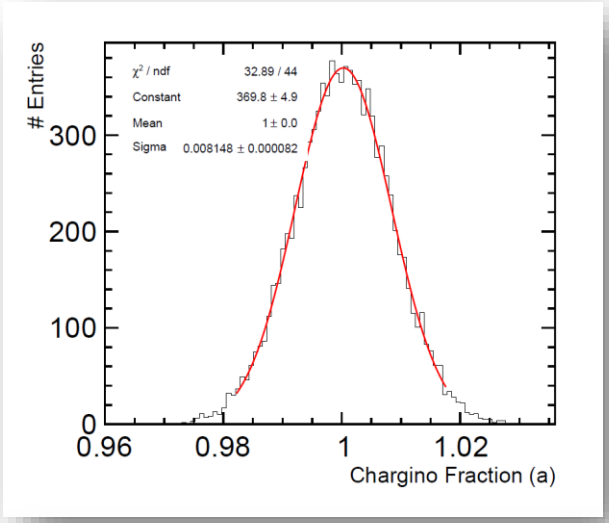

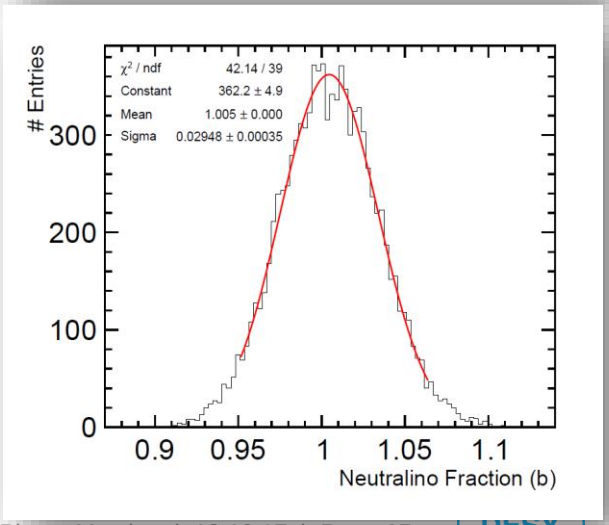

Conclusions

- The performance of SGV-PFL was investigated:
  - In terms of **visible energy** → the shift to higher energies addressed by scaling the neutral PFO energy
  - In terms of **JER** → 50-60% worse than DBD performance
  - Considered “pessimistic scenario” → investigated effect on “point 5” analysis
- The “point 5” mass and cross-section determination performed on SGV-PFL data samples:
  - SGV-PFL results well compatible with LoI and DBD
  - Large difference in PandoraPFA-style JER not visible on analysis level due to jet finding effects and jet-level confusion
  - Use of kinematic fit most likely reduces sensitivity to JER

Thank You!

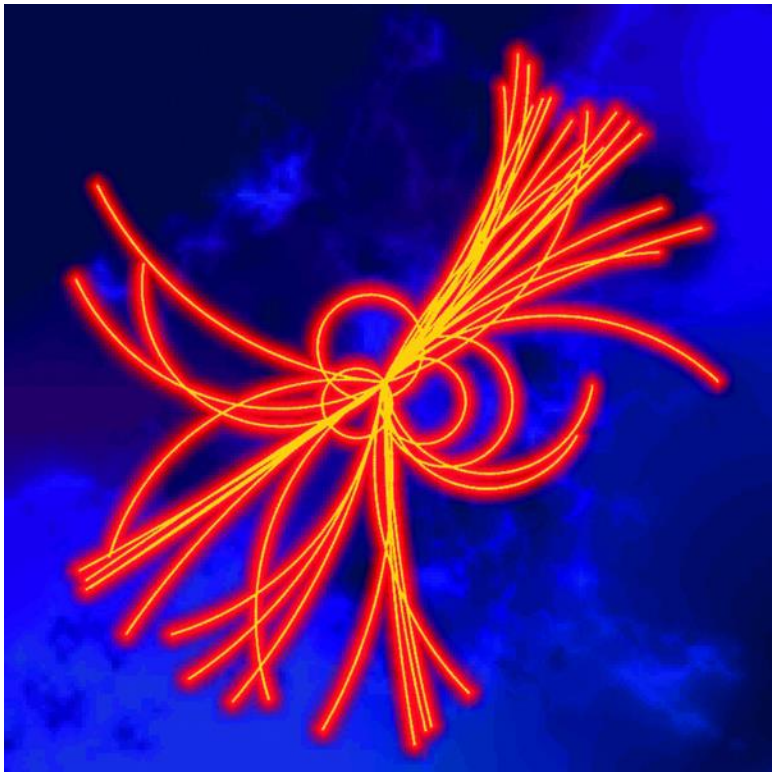

Back-up Slides

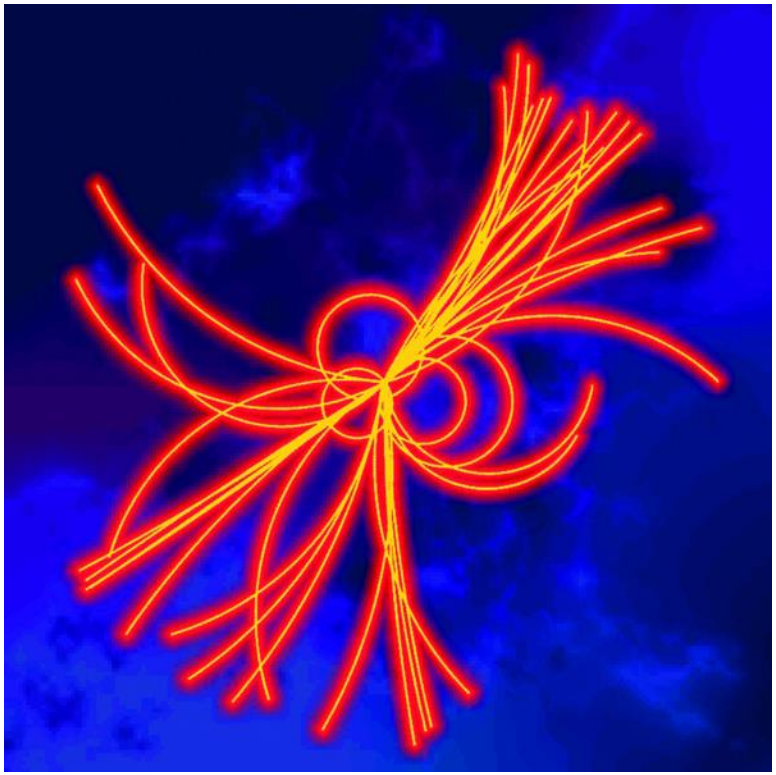

Study Case - Motivation

- Signal topology:
  - Four jets and missing energy (due to LSP)
  - Hadronic decay modes of gauge bosons chosen as signal
  - Both decay channels treated as signal in turn

$$\tilde{\chi}_1^{\pm} \rightarrow \tilde{\chi}_1^0 W^{\pm} \quad \text{and} \quad \tilde{\chi}_2^0 \rightarrow \tilde{\chi}_1^0 Z^0$$

- $\tilde{\chi}_1^{\pm}$ and $\tilde{\chi}_2^0$ sample separation: essentially distinguish between W and Z pair events
- **Challenge detector and particle flow performance**

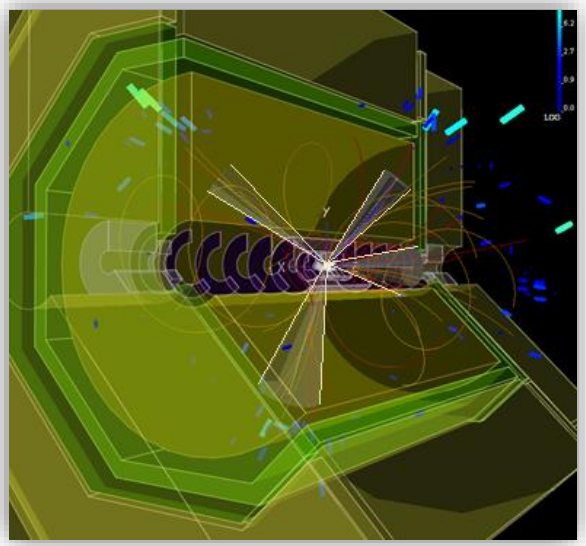

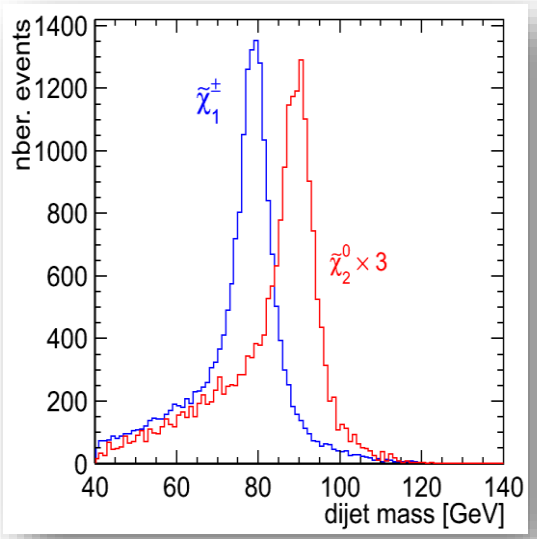

Data Samples:

- Signal: 40000 $\tilde{\chi}_1^{\pm}$ events and 9000 $\tilde{\chi}_2^{0}$ events

LOI sample:	**DBD sample:**
Signal generated with `Whizard1.51` Background generated with `Whizard1.40`	Signal (as well as SM background) generated with `Whizard 1.95`
The RDR beam spectrum was used	The TDR beam spectrum was used
	Some processes could not be produced in Whizard 1.95
Signal + background were simulated and reconstructed with `ilcsoft v01-06`	Signal + background were simulated and reconstructed with `ilcsoft v01-16-02`
The jet energy scale was increased by 1%	The jet energy scale was **not** increased
No $\gamma\gamma$ background overlay	The **$\gamma\gamma$ background overlay** was taken into account
The analysis was run on existing data samples	The analysis was run

- **Note:** in the signal samples, the M_W was inadvertently lowered by Whizard to M_W = 79.8 GeV

Analysis Strategy

- Remove $\gamma\gamma \rightarrow hadrons$ background: applied k_T exclusive algorithm $\leftrightarrow$ 6 jets, R=1.1 (FastJet)
- Cluster event into 4 jets (Durham)
- Run kinematic fit (equal mass constraint: $M_{jj1} = M_{jj2}$)
  - → choose jet pairing with best fit probability
- Run isolated lepton finder (J. Tian and C. Dürig)
- Perform SUSY selection (12/16 cuts → see back-up slide)

Sample	$\tilde{\chi}_1^{\pm}$ hadronic	$\tilde{\chi}_2^0$ hadronic
Efficiency	90.8% → 53%	91% → 30%
Purity	14.7% → 63%	2.6% → 38%
Efficiency	72%	73%
Purity	27%	5%

Selection for mass

Selection for x-section

Analysis Strategy

- Remove $\gamma\gamma \rightarrow hadrons$ background: applied k_T exclusive algorithm $\leftrightarrow$ 6 jets, R=1.1 (FastJet)

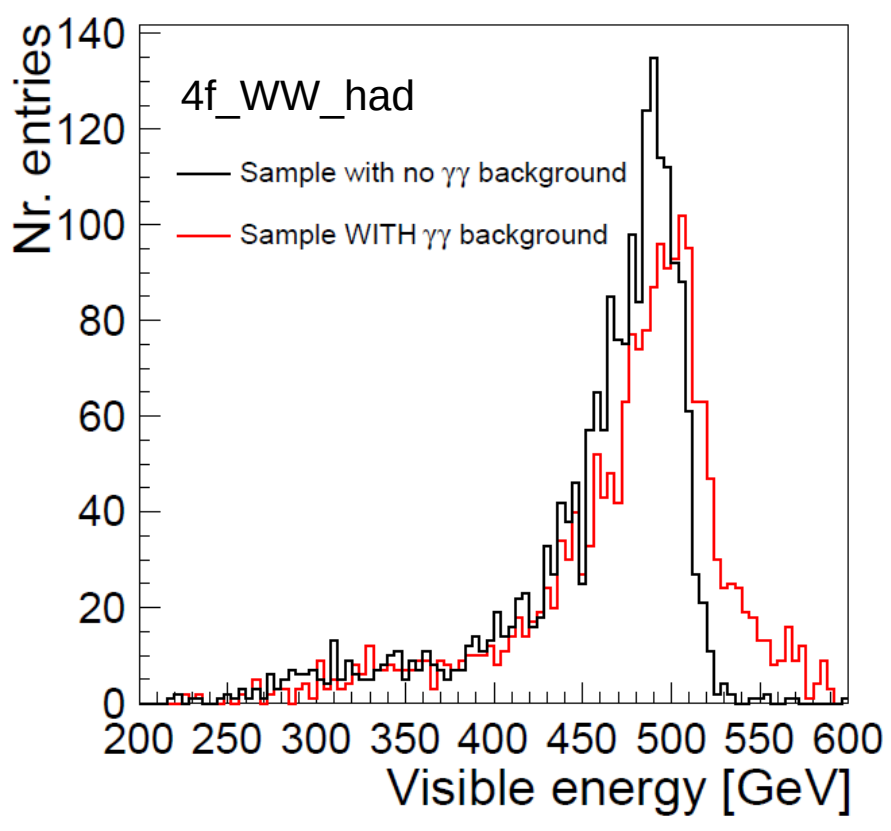

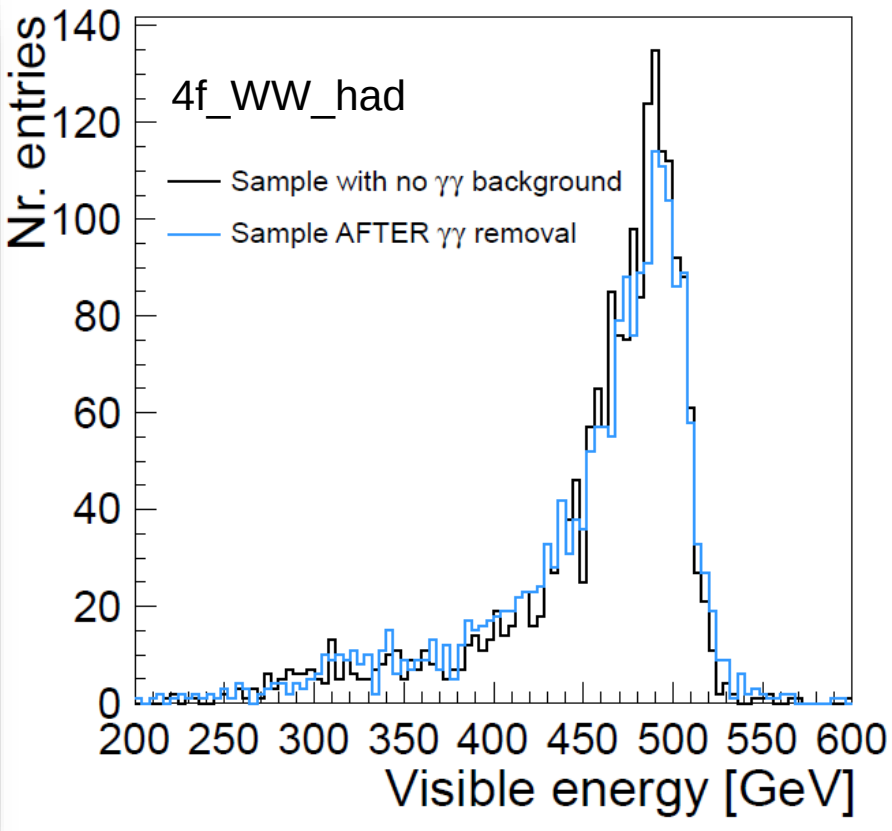

Cutflow

Sample	$\tilde{\chi}_1^{\pm}$ hadronic (signal)	$\tilde{\chi}_2^0$ hadronic (signal)	SUSY background	$\gamma\gamma$ & γe (SM)	2 fermions (SM)	4 fermions (SM)	6 fermions (SM)
No cut	27427	4897	71450	173791	1.1239e+07	1.60385e+07	589188
No isolated leptons found	27281	4857	39592	51136	1.02105e+07	9.21406e+06	372419
Nber. PFOs in event	27274	4853	28936	38553	8.61602e+06	6.73891e+06	311637
Nber. tracks with $P_T > 1$ GeV in event	27228	4851	25530	34803	7.60753e+06	6.22246e+06	282188
Thrust	27213	4845	24996	34347	4.57776e+06	4.9343e+06	281913
Nber. tracks in event	27193	4841	23049	33647	4.27554e+06	4.81107e+06	281652
Visible energy	27159	4831	20935	21830	2.88111e+06	926895	17059
Jet energy	27141	4829	17895	21360	2.55856e+06	846448	16914
Jet cos(θ)	26530	4729	15964	17582	1.78384e+06	607998	16049
y_{34}	26372	4704	11202	16231	330943	299658	14892
Nber tracks in jet	25434	4585	8083	14666	261520	205867	12125
Miss cos(θ)	25171	4535	8020	4489	9171	117756	11656
Lepton energy	24913	4460	7749	4281	8432	109365	10121
Nber. PFOs in jet	24737	4444	7305	4148	8253	102304	9783
Miss cos(θ)	19868	3589	6135	1383	1100	53957	6955
Missing mass	19830	3584	6134	1175	931	41326	1764
Kinematic fit converged	19753	3565	5966	1152	839	40263	1749

Blue: selection for the mass measurement
Red: selection for the cross section measurement

Mass Measurements

$\tilde{\chi}_1^{\pm}$ and $\tilde{\chi}_2^0$ Signal Separation

- Calculate χ^2 with respect to nominal W / Z mass

$$\chi^2(m_{j1}, m_{j2}) = \frac{(m_{j1} - m_V)^2 + (m_{j2} - m_V)^2}{\sigma^2}$$

⇩

min $\chi^2 \rightarrow \tilde{\chi}_1^{\pm}$ and $\tilde{\chi}_2^0$ separation

- Downside: lose statistics
  - Cut away 47% of $\tilde{\chi}_1^{\pm}$ surviving events
  - Cut away 61% of $\tilde{\chi}_2^0$ surviving events
- However, after the χ^2 cut, the separation is quite clear:

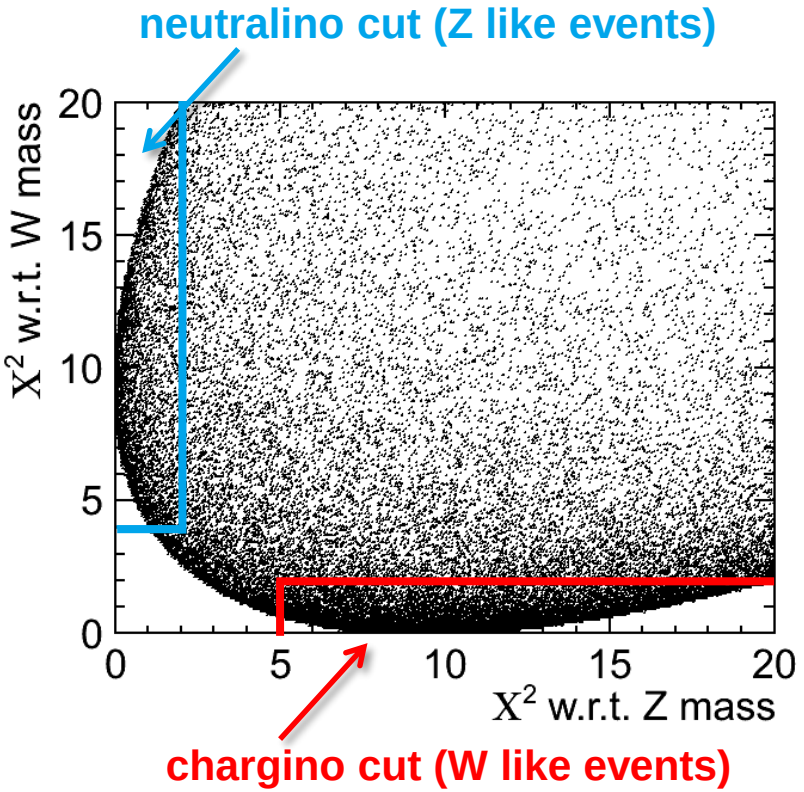

Sample	$\tilde{\chi}_1^{\pm}$ hadronic	$\tilde{\chi}_2^0$ hadronic
Efficiency	90.8%	91%
Purity	14.7%	2.6%

Obs.	DBD	
	$\tilde{\chi}_1^{\pm}$	$\tilde{\chi}_2^0$
Efficiency	53%	30%
Purity (total)	63%	38%
Purity (SUSY)	94%	62%

Gaugino Mass Measurement

- Mass difference to LSP ($\tilde{\chi}_1^0$) is **larger** than M_Z → decays of real gauge bosons
- This is a **two-body decay** (well known kinematics!)

- In the gaugino C.M frame: *(E, p conservation)*

$$\boldsymbol{P}_\chi = \boldsymbol{P}_V + \boldsymbol{P}_{LSP} \Rightarrow \boldsymbol{P}_{LSP} = \boldsymbol{P}_\chi - \boldsymbol{P}_V$$

where $\boldsymbol{P}_\chi = (M_\chi, \vec{0})$

$$M_{LSP}^2 = M_\chi^2 + M_V^2 - (2E_\chi E_V - \vec{p}_V \vec{p}_\chi)$$

$$\boldsymbol{E_V = (M_\chi^2 + M_V^2 - M_{LSP}^2)/2M_\chi} \quad \textbf{(boson energy)}$$

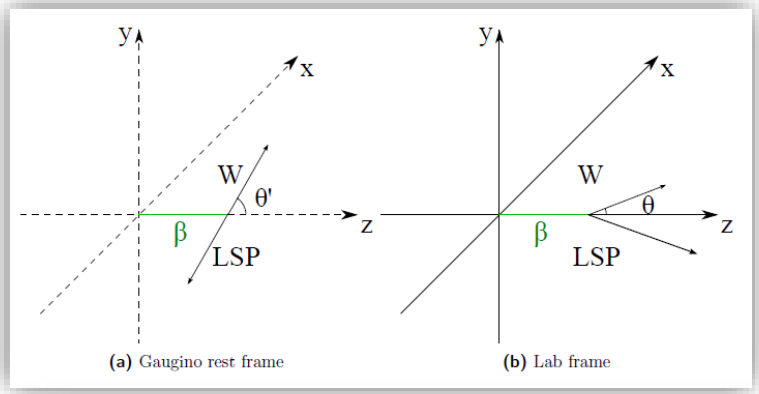

- Boosting into the lab frame:

$$E_V^{lab} = \gamma E_V + \beta\gamma \vec{p}_{V,\parallel}$$
$$= \gamma E_V + \beta\gamma |\vec{p}_V| \cos\theta'$$

$$\theta' = 0 \rightarrow E_V^{lab} = \gamma E_V + \beta\gamma \sqrt{E_V^2 - M_V^2}$$

$$\theta' = \pi \rightarrow E_V^{lab} = \gamma E_V - \beta\gamma \sqrt{E_V^2 - M_V^2}$$

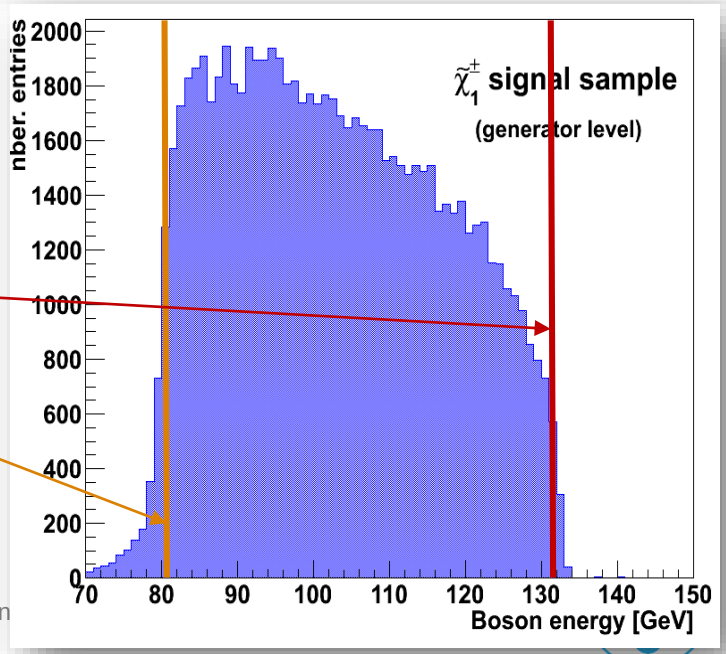

- **Use edge values to calculate gaugino masses!**
- **Two** different **strategies** for edge detection

LOI Strategy: Fit the Boson Energy Spectrum

- Fit dijet energy spectrum and obtain edge positions:

$$f(x; t_{0\_1}, b_{0\_2}, \sigma_{1\_2}, \gamma) = f_{SM} + \int_{t_0}^{t_1} (b_2 t^2 + b_1 t + b_0) V(x - t, \sigma(t), \gamma) dt$$

- The only free fit parameters: the edge positions t_0 and t_1
- Polynomial → Spectrum slope
- Voigt function → detector resolution and gauge boson width

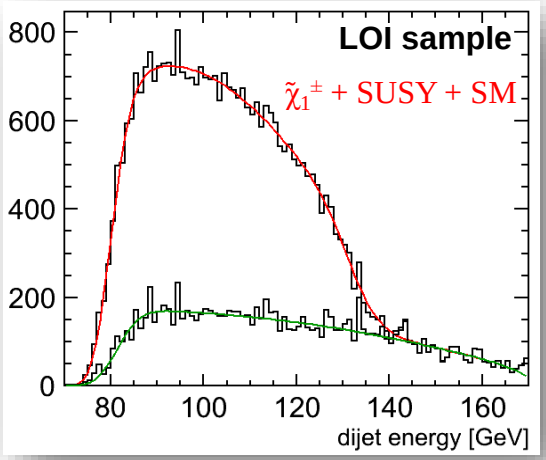

- Issues with the LOI method:

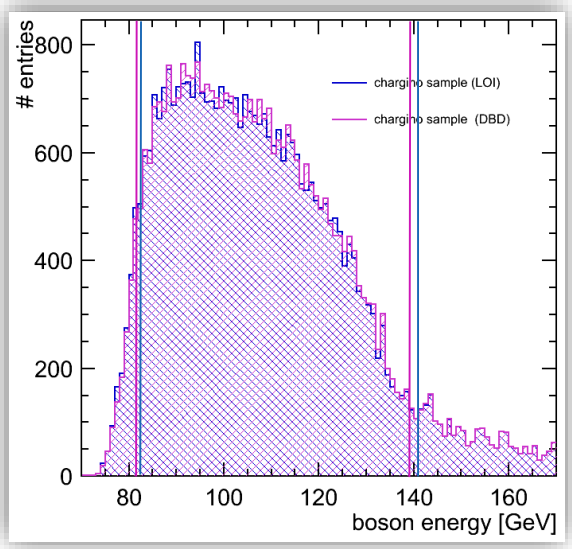

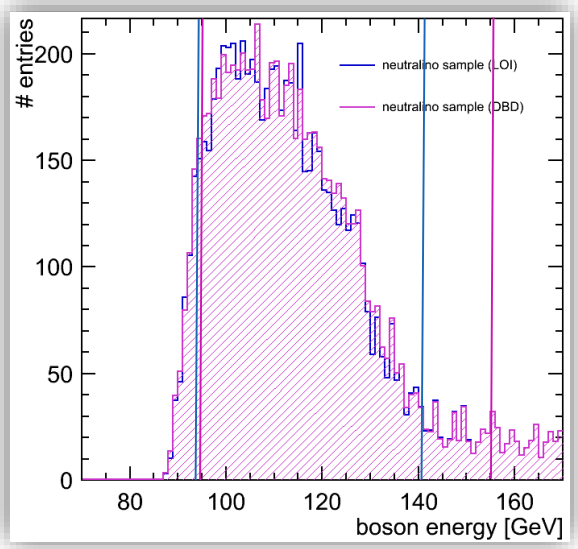

Fit method highly sensitive to small fluctuations in energy distribution.

Apply a different edge extraction method!

DBD Strategy: Endpoint Extraction using an FIR Filter

- Finite Impulse Response (FIR) filters are digital filters used in signal processing.
- FIR filters can operate both on discrete as well as continuous values.
- The concept of “finite impulse response“ ↔ **the filter output** is computed as a finite, weighted sum of a finite number of values from the filter input.

$$y[n] = \sum_{k=-M_1}^{M_2} b_k x[n-k]$$

the input signal

the filter coefficients (weights)

- y is obtained by convolving the input signal with the (finite) weights

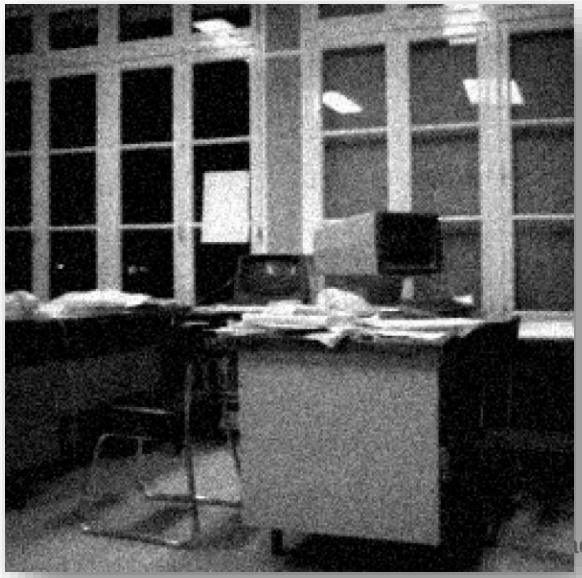

D. Demigny, T. Kamlé

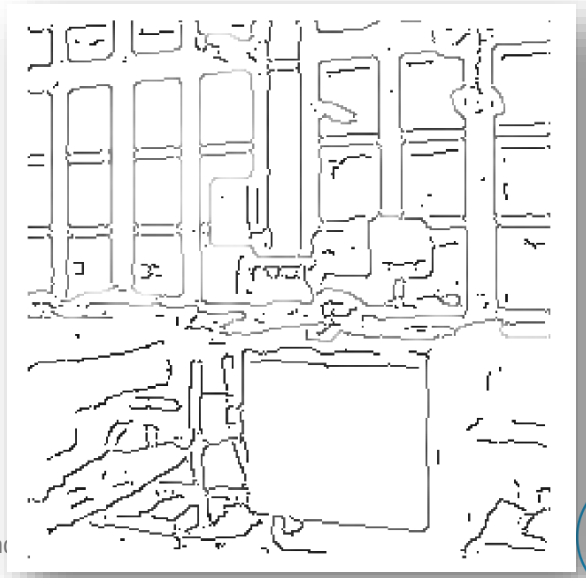

Choosing the Appropriate Filter

- Canny's criteria for an optimal filter:
  - *J. F. Canny*. **A computational approach to edge detection.** *IEEE Trans. Pattern Analysis and Machine Intelligence*, pages 679-698, 1986
  - **Good detection**: probability of obtaining a peak in the response must be high
  - **Localisation**: standard deviation of the peak position must be small
  - **Multiple response minimisation**: probability of false postive detection must be small
- Canny has shown that an optimal filter is very similar to the first derivative of a Gaussian

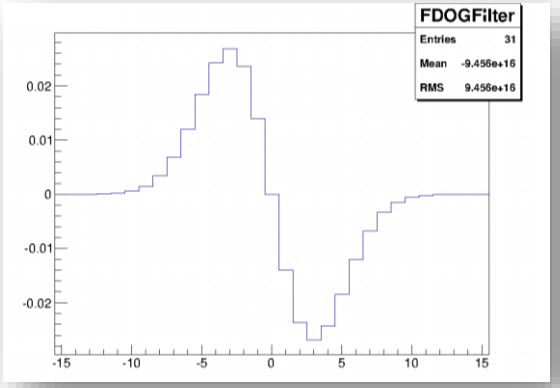

- There are 3 filter parameters that can be optimised (via toy Monte Carlo)
  - The width of the Gaussian (σ) = **4**
  - The kernel size (# bins of the filter histogram) = **17**
  - The binning of the input boson energy histogram = **1 GeV/bin**
- Edge positions stable within max.1.8% when varying filter parameters
- (Reminder: LOI edge fluctuations [from LOI vs DBD comparison]: 9.4%)

Applying an FIR Filter

- Goal: find edge positions in spectrum

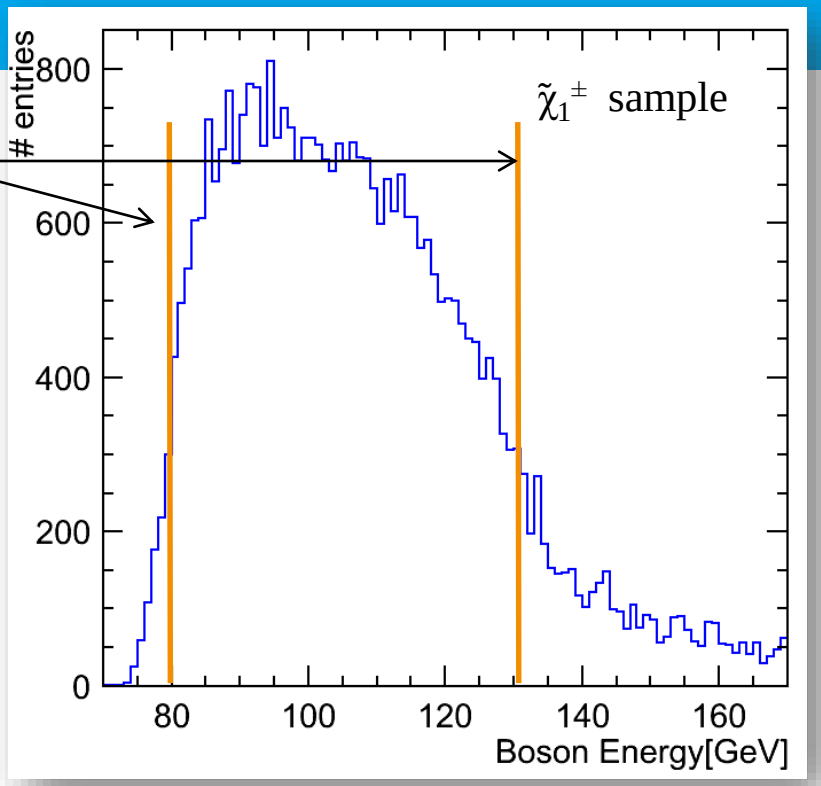

Applying an FIR Filter

Thanks to S. Caiazza.

- Goal: find edge positions in spectrum
- Strategy:
  - Choose an FIR filter (kernel)
  - Note: filter length << signal histogram length
  - Treat both signal histogram as well as filter as **arrays**:

Bin #	1	2	3	...	98	99	100
Signal	0	15	28	...	34	22	4

Bin #	1	2	3	...	28	29	30
Filter	0	0.01	0.02	...	-0.02	-0.01	0

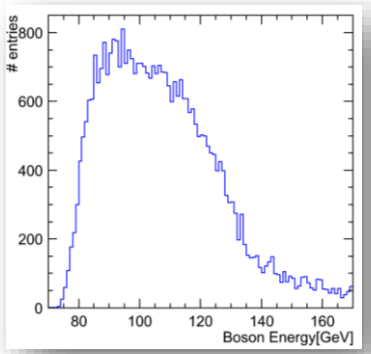

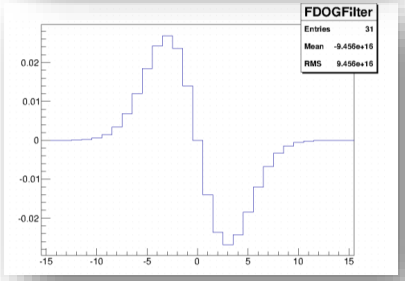

Applying an FIR Filter

- Goal: find edge positions in spectrum
- Strategy:
  - Choose an FIR filter (kernel)
  - Note: filter length << signal histogram length
  - Treat both signal histogram as well as filter as **arrays**
  - Calculate dot product between **Signal** and **Filter → obtain one value**

Bin #	1	2	3	...	98	99	100
Signal	0	15	28	...	34	22	4

Bin #	1	2	3	...	28	29	30
Filter	0	0.01	0.02	...	-0.02	-0.01	0

$$0 \times 0 \; + \; 0.01 \times 15 \; + \; 0.02 \times 28 \; + \ldots \; = \text{val1}$$

Applying an FIR Filter

- Goal: find edge positions in spectrum
- Strategy:
  - Choose an FIR filter (kernel)
  - Note: filter length << signal histogram length
  - Treat both signal histogram as well as filter as arrays
  - Calculate dot product between Signal and Filter → obtain one value

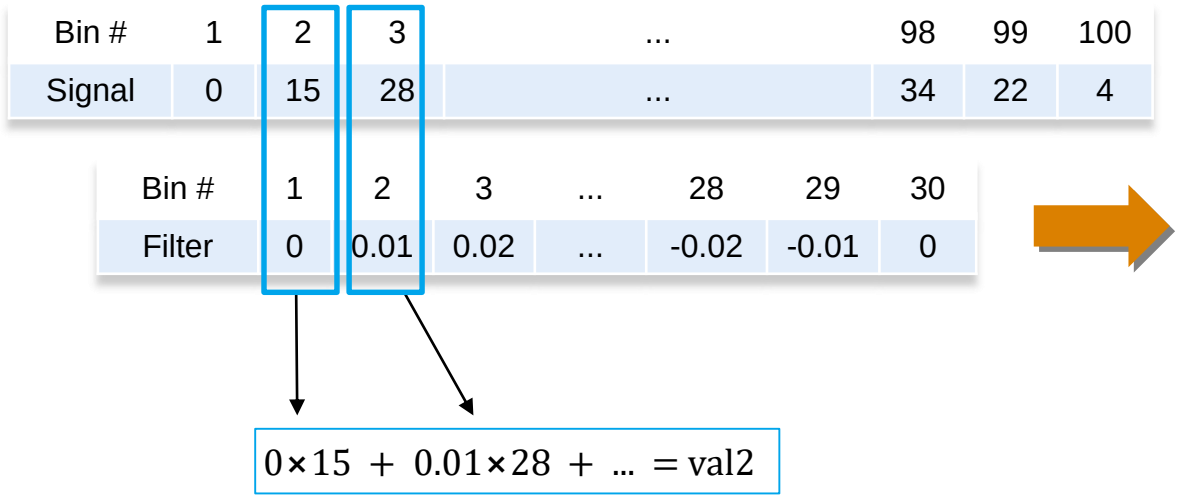

  - **"Move" Filter along the (length) of the signal → obtain more values, which will form the total filter response**

Applying an FIR Filter

- Goal: find edge positions in spectrum
- Procedure:
  - Choose an FIR filter (kernel)
  - Note: filter length << signal histogram length
  - Treat both signal histogram as well as filter as arrays
  - Calculate dot product between Signal and Filter → obtain one value

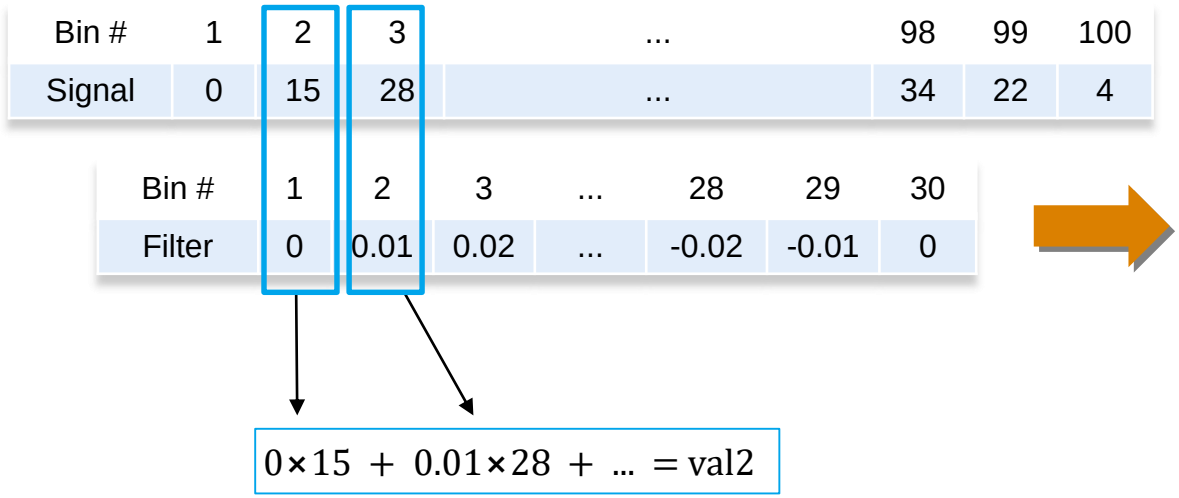

  - **"Move" Filter along the (length) of the signal → obtain more values, which will form the total filter response**

FDOG Filter Optimisation

- There are 3 filter parameters that can be optimised
  - The width of the Gaussian (σ)
  - The kernel size (# bins of the filter histogram)
  - The binning of the input boson energy histogram

FDOG Filter Optimisation

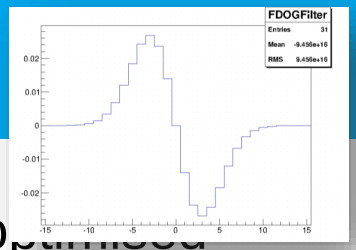

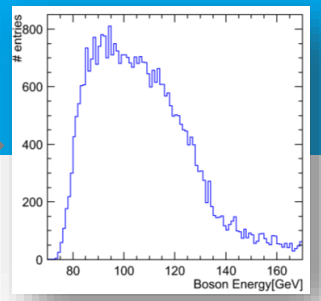

- There are 3 filter parameters that can be optimised
  - **The width of the Gaussian (σ)** ***(the kernel and bin sizes were fixed)***
  - The kernel size (# bins of the filter histogram)
  - The binning of the input boson energy histogram

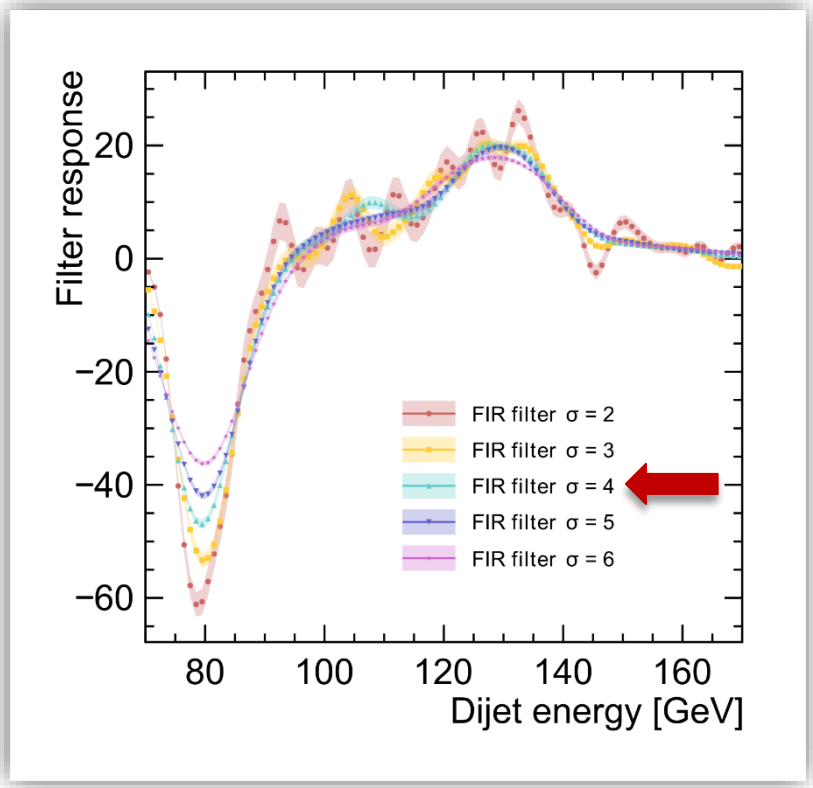

FDOG Filter Optimisation

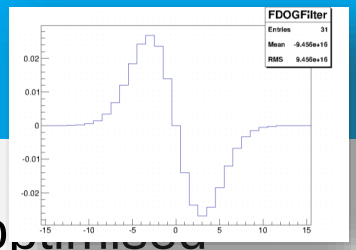

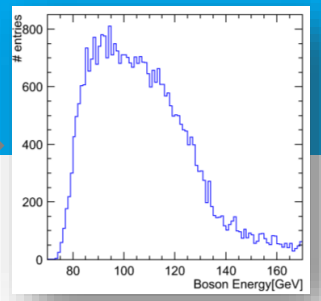

- There are 3 filter parameters that can be optimised
  - The width of the Gaussian (σ) = 4
  - **The kernel size (# bins of the filter histogram)** ***(the σ and bin sizes were fixed)***
  - The binning of the input boson energy histogram

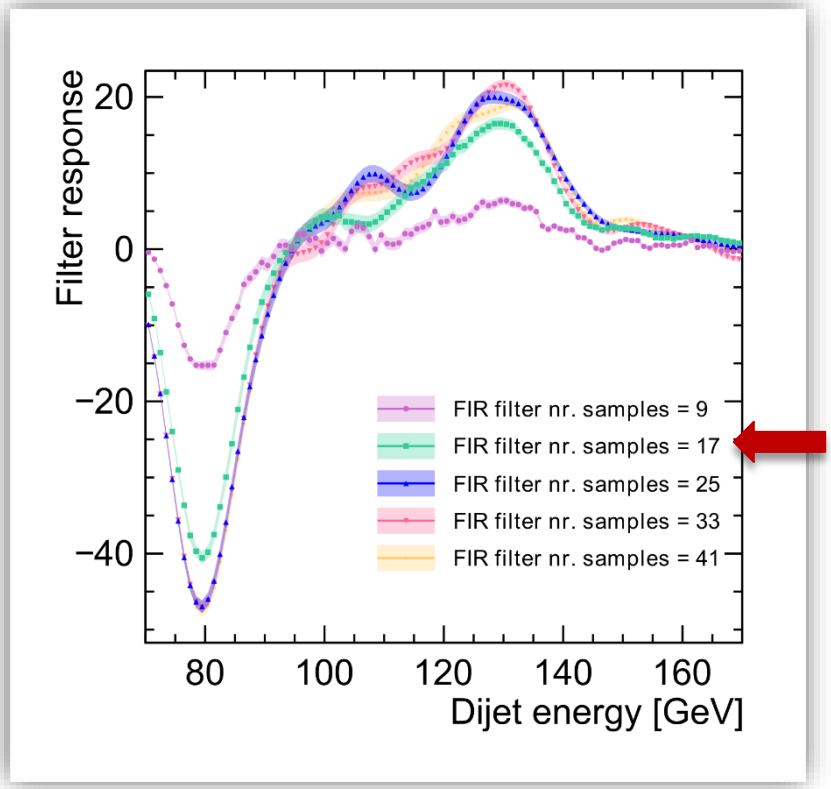

FDOG Filter Optimisation

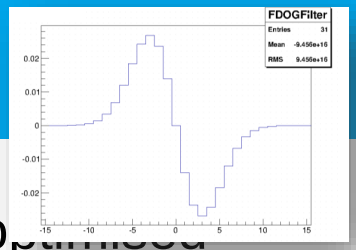

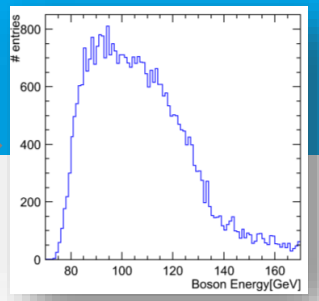

- There are 3 filter parameters that can be optimised
  - The width of the Gaussian (σ) = 4
  - The kernel size (# bins of the filter histogram) = 17
  - **The binning of the input boson energy histogram** ***(the σ and kernel sizes were fixed)***

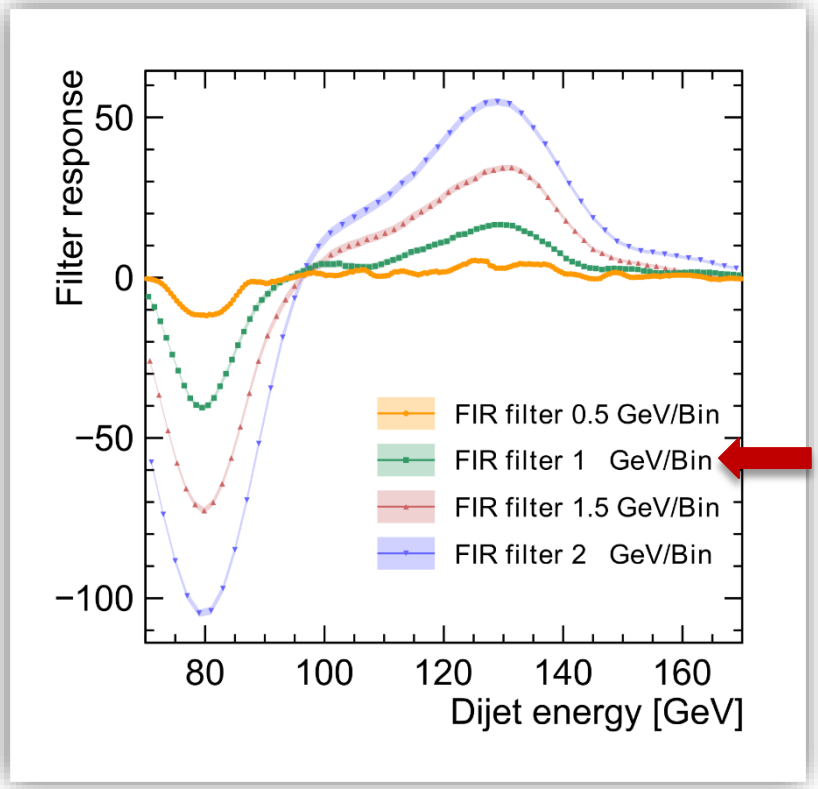

Applying the FIR Filter on DBD Data: Results

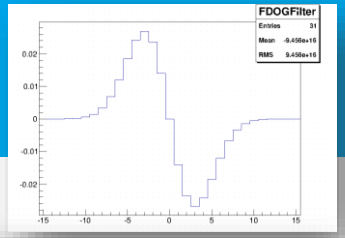

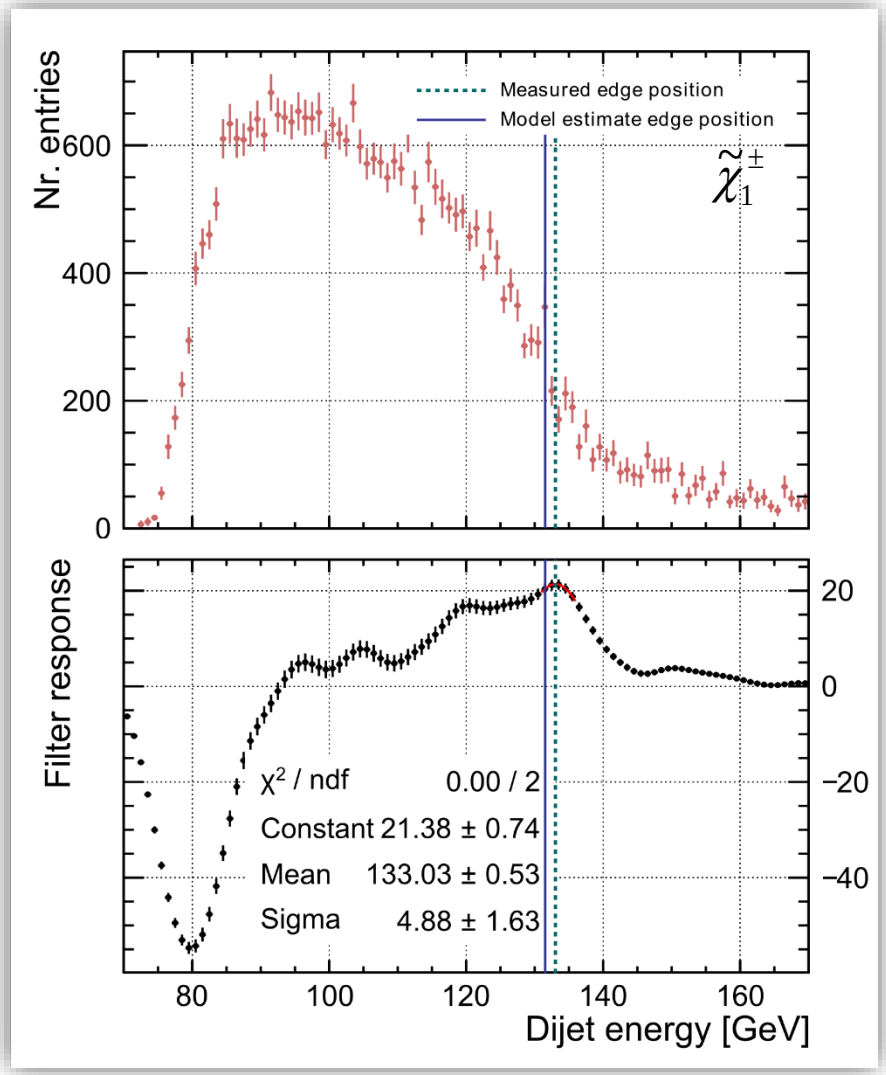

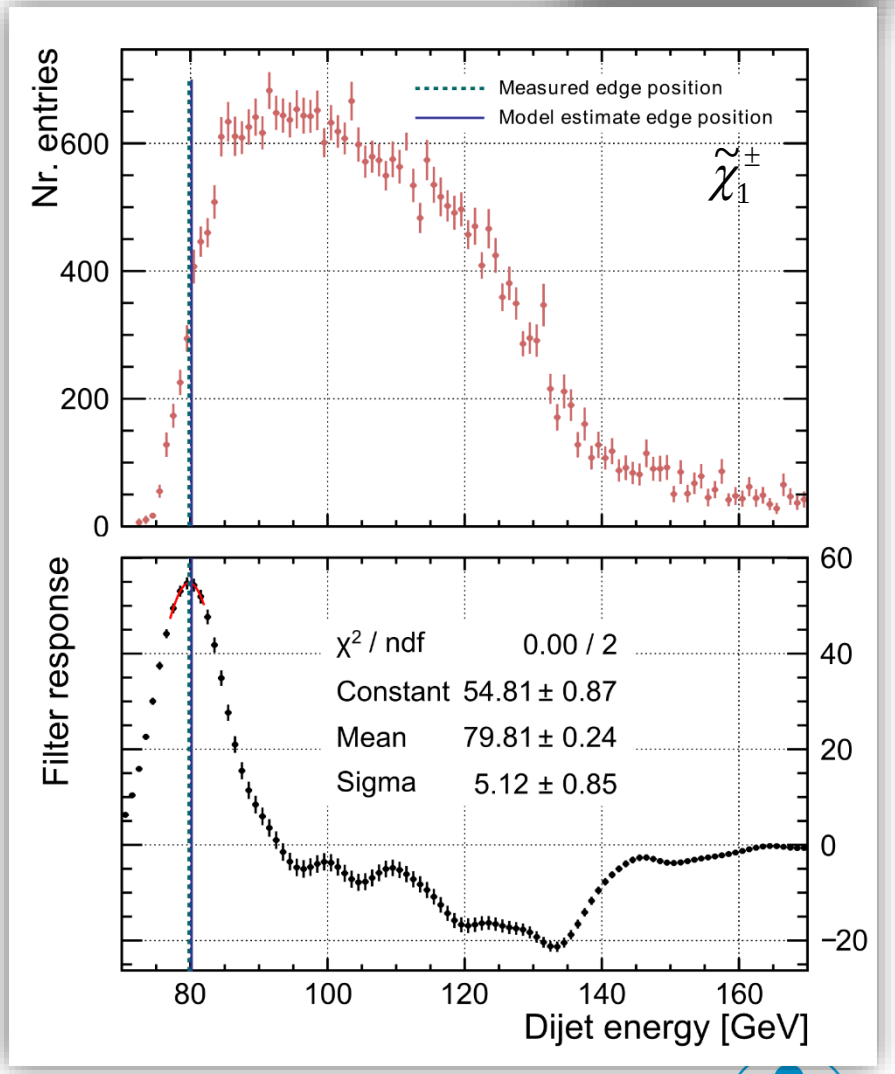

Edge Extraction Comparison

True	80.17	131.53	93.24	129.06
Sim.	**Edge W_{low} [GeV]**	**Edge W_{high} [GeV]**	**Edge Z_{low} [GeV]**	**Edge Z_{high}[GeV]**
LOI	80.4±0.2	129.9±0.7	92.3±0.4	128.3±0.9
DBD	79.6±0.2	130.1±0.8	92.1±0.3	128.9±0.8

filter

Sample	Mass $\tilde{\chi}_1^{\pm}$ [GeV]	Mass $\tilde{\chi}_2^0$ [GeV]	Mass $\tilde{\chi}_1^0$ [GeV]
TRUE	**216.5**	**216.7**	**115.7**
LOI	216.9±3.2	220.0±1.4	118.4±1.1
DBD	216.8±3.2	220.6±1.2	118.2±0.9

- The filter method is more stable in determining the edge position
- The mass values extracted from the LOI and DBD samples: well compatibile within their statistical errors
- The systematic errors will be addressed by a **mass calibration study**

DESY

Cross Section Measurement

Cross Section Determination Method

- Interested in: $\sigma(e^+e^- \to \tilde{\chi}_1^+\tilde{\chi}_1^-) \times \mathrm{BR}\,(\tilde{\chi}_1^+\tilde{\chi}_1^- \to \tilde{\chi}_1^0\tilde{\chi}_1^0 W^+W^-)$
  $\sigma(e^+e^- \to \tilde{\chi}_2^0\tilde{\chi}_2^0) \times \mathrm{BR}(\tilde{\chi}_2^0\tilde{\chi}_2^0 \to \tilde{\chi}_1^0\tilde{\chi}_1^0 Z^0Z^0)$
- Relevant observable: the reconstructed dijet [boson] mass
- Relevant distribution: the reconstructed mass of one dijet pair versus the other:
  - **AFTER** applying all selection cuts
  - Considering only those events for which the kinematic fit has converged
  - Including **all** possible dijet associations

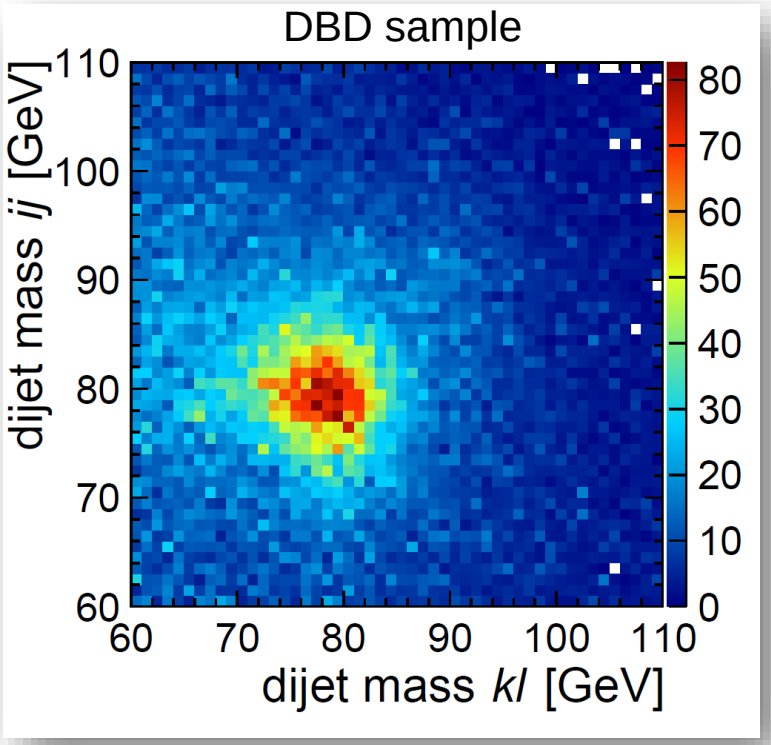

The total distribution (SUSY + SM)

- Since $\sigma \propto \frac{Nr.events}{\varepsilon \cdot \int \mathcal{L}} \Rightarrow$ the goal is to identify the number of $\tilde{\chi}_1^{\pm}$ and $\tilde{\chi}_2^0$ events from the total distribution

→ Perform 2D Template fit.

Cross Section: 2D Template Fit

- Use Monte Carlo data to produce:
  - the chargino template

- After preselection
- Kinematic fit converged
- All dijet permutations included

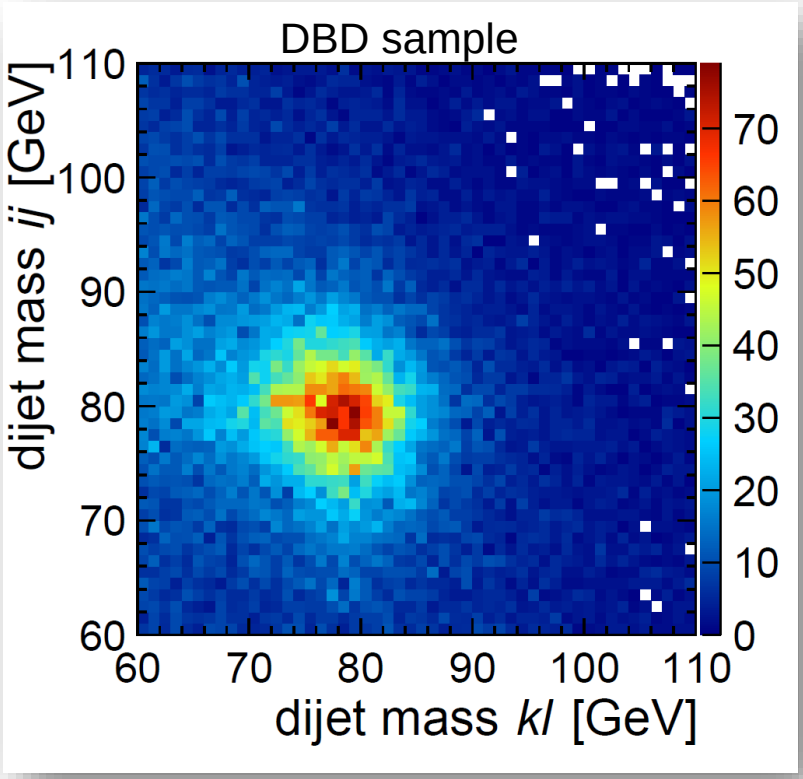

Chargino events only

Cross Section: 2D Template Fit

- Use Monte Carlo data to produce:
  - the chargino template
  - the neutralino template

- After preselection
- Kinematic fit converged
- All dijet permutations included

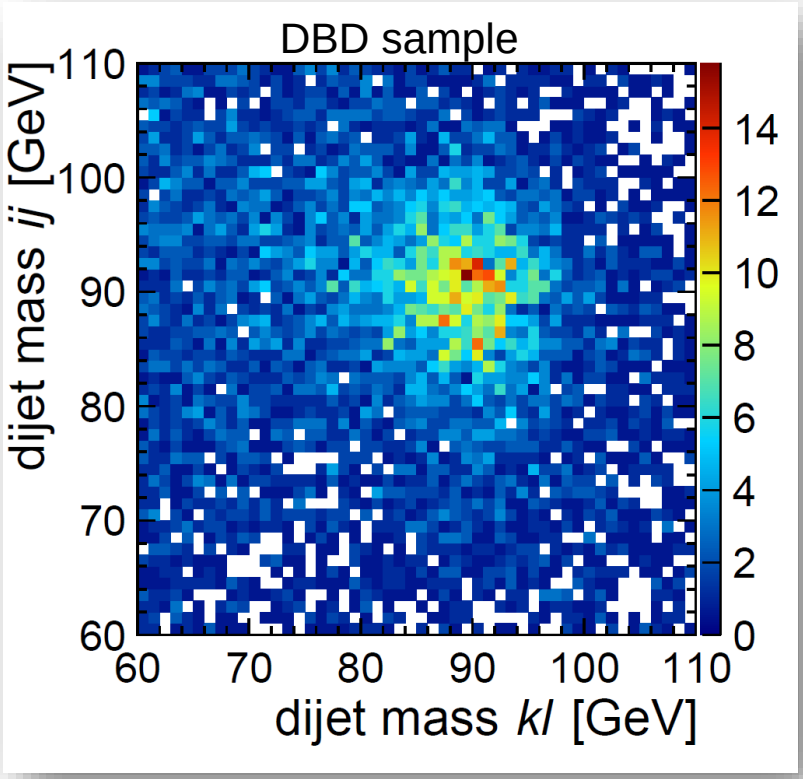

Neutralino events only

Cross Section: 2D Template Fit

- Use Monte Carlo data to produce:
  - the chargino template
  - the neutralino template
  - the SM background template

- After preselection
- Kinematic fit converged
- All dijet permutations included

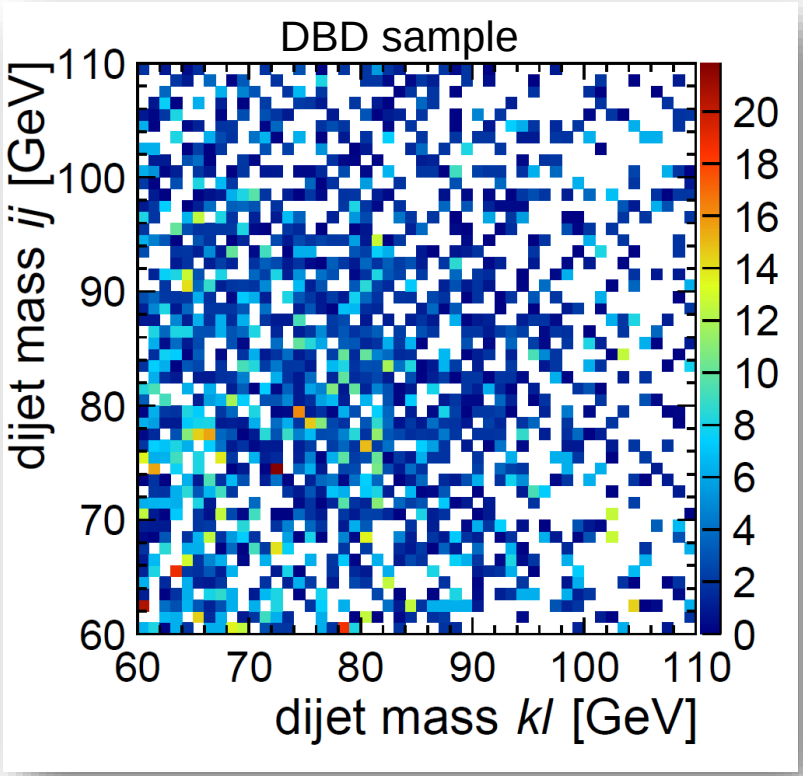

Standard Model events only

Cross Section: 2D Template Fit

- Use Monte Carlo data to produce:
  - the chargino template
  - the neutralino template
  - the SM background template
  - the SUSY background → **negligible**!

- After preselection
- Kinematic fit converged
- All dijet permutations included

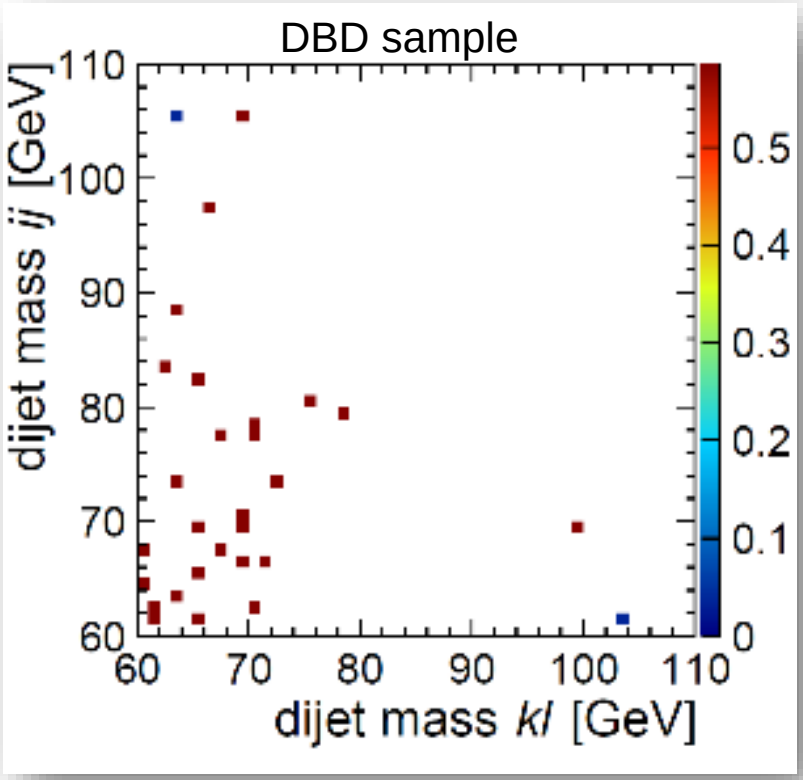

SUSY background events only

Cross Section: 2D Template Fit

- The fitting procedure:

> Subtract the SM background template from the total data distribution

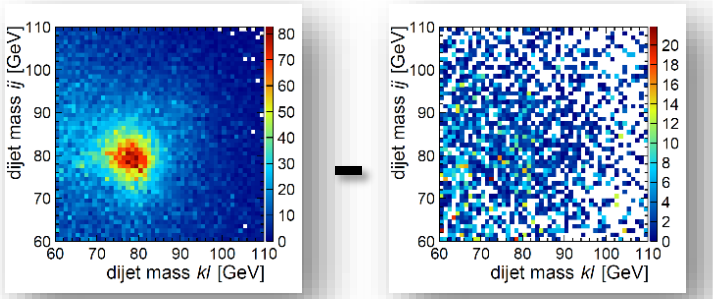

> Defining the two-dimensional fitting function:

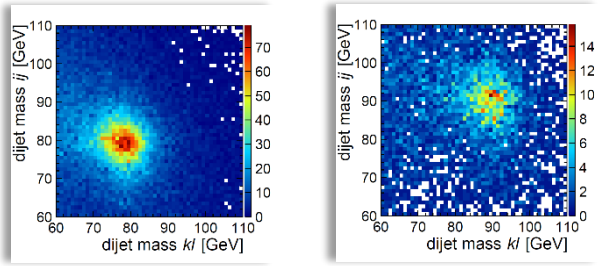

$$f_{Fit}(x,y) = a \cdot f_{\tilde{\chi}_1^{\mp}}(x,y) \; + \; b \cdot f_{\tilde{\chi}_2^{0}}(x,y)$$

- a and b → the only free parameters
- a and b = the fraction of template events found in the total data distribution
- in an ideal case, a = b =1

> Apply the template fit on the remaining data events

2D Template Fit Toy Monte Carlo

- **Note:** limited amount of Monte Carlo data available → **toy Monte Carlo study**
- **Running the toy MC**:
  - Treat the total data distribution as a p.d.f
  - Randomly sample the initial distribution N times: $N = N_{evts.}^{initial} \pm \sqrt{N_{evts.}^{initial}}$
  - Subtract the SM template from the new distribution
  - Apply the fitting function → obtain one value each for a and b
  - Repeat procedure 10000 times

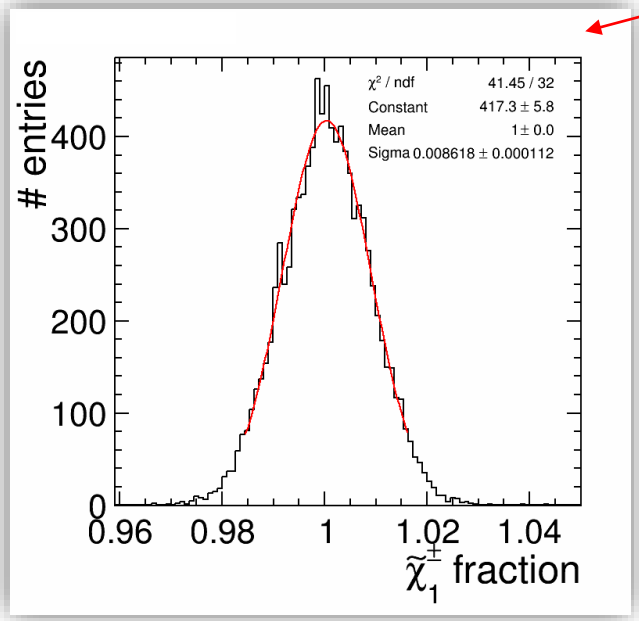

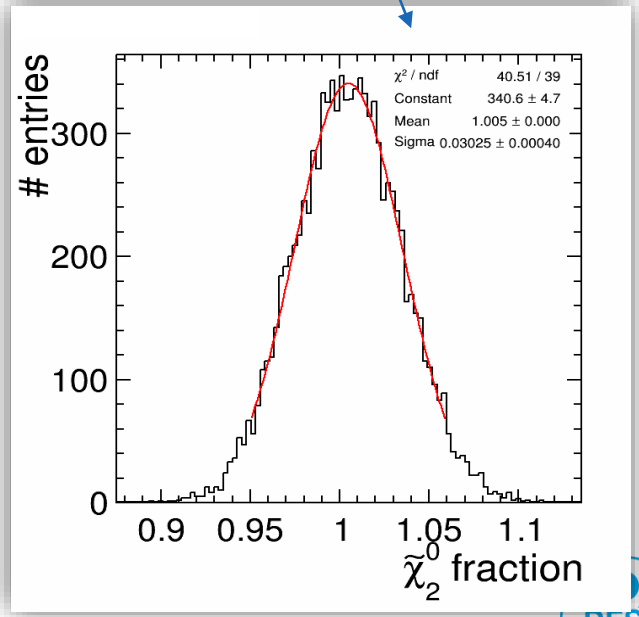

2D Template Fit: Results

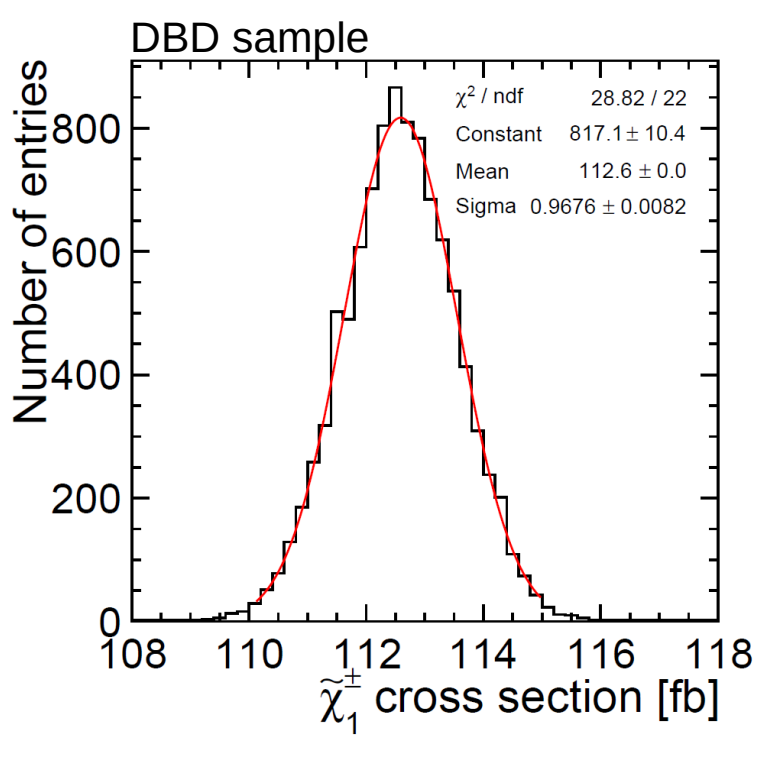

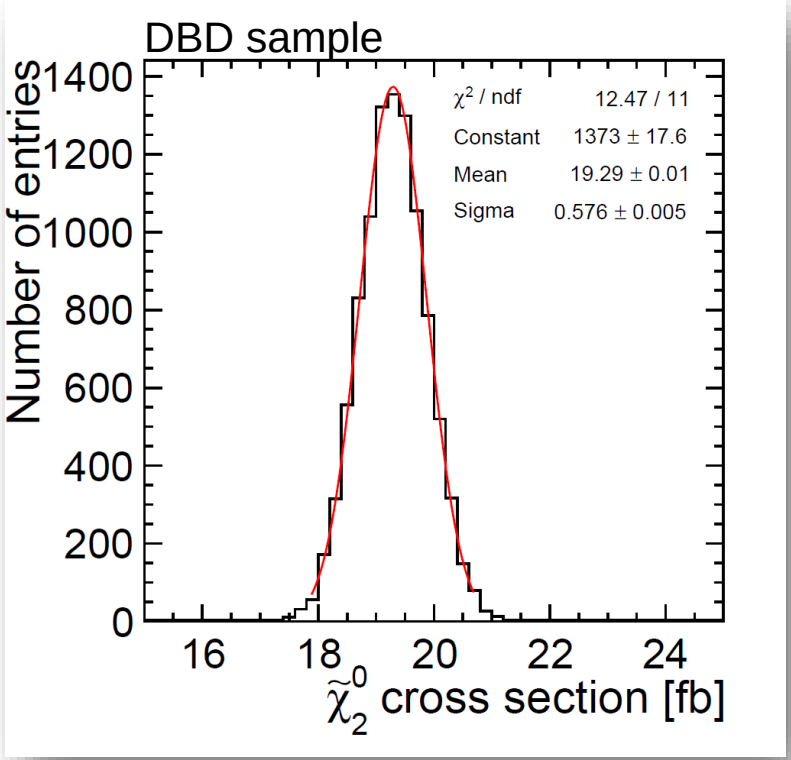

$$a_{mean} = 1.00 \pm 0.009$$
$$b_{mean} = 1.01 \pm 0.03$$

Sample	$\tilde{\chi}_1^{\pm}$ x- section [fb]	$\tilde{\chi}_2^0$ x-section [fb]
Generator	112.54	19.2
DBD	112.6 ± 0.97	19.3 ± 0.58

Cross Section: 2D Template Fit – Comparison to LOI

- The same procedure has been applied to the LOI data:

Sample	$\tilde{\chi}_1^{\pm}$ x- section [fb]	$\tilde{\chi}_2^0$ x-section [fb]
Generator level	132.2	22.8
LOI	132.2 $\pm$1.1	23.2 $\pm$0.7
arXiv:0906.5508v2	132.9 $\pm$ 0.9	22.5 $\pm$ 0.5

Sample	$\tilde{\chi}_1^{\pm}$ x- section [fb]	$\tilde{\chi}_2^0$ x-section [fb]
Generator level	112.5	19.2
DBD	112.6 $\pm$ 0.97	19.3 $\pm$ 0.6

- **Note** - the difference between cross sections at generator level
  - Difference in beam-spectrum
  - Missing processes - Whizard 1.95